Random-field systems, spin glasses and vertex covers: on the relation of statistical physics and combinatorial optimization

Kumulative Habilitationsschrift
zur Erlangung der venia legendi im Fach Physik

vorgelegt der Fakultät für Physik
der Georg-August Universität Göttingen

Alexander Karl Hartmann
Institut für Theoretische Physik
Georg-August Universität Göttingen

Göttingen 2004

Preface

This text gives an overview of the central topics of the work of the author in the years from 1998 to 2003 and states the main achievements he contributed to. A a selection of his research papers can be found reprinted in the appendix.

The author works at the interface of physics and computer science. On one hand, he applies recently developed efficient algorithms, especially optimization algorithms, to study disordered physical systems numerically, namely random-field systems and spin glasses. These fast algorithms were developed during the last decade in computer science. The author developed in addition some heuristics which allow to study much larger sizes than before.

On the other hand, he studied numerically combinatorial optimization problems, which play a fundamental role in theoretical computer science. Using concepts and methods from statistical physics he investigated the vertex-cover problem, which is treated in this text, but also the satisfiability problem, which is beyond the scope of this text. Both problems belong to the six basic so called NP-complete problems, which play a crucial role for complexity theory in computer science.

Hence, although the models studied here originate from different fields, they are linked by combinatorial optimization. For the disordered physical systems, classical ground states of the models are calculated, i.e. the minimum-energy states. The problems studied in theoretical computer science are idealizations of optimization problems occuring in everyday life, e.g. the minimization of the number of guards in a museum or the minimization of the length of a closed tour connecting different cities.

The physical models studied here, random-field systems and spin glasses, are models for disordered magnetic alloys. Beginning in the 1970s, the low-temperature behavior of these systems was studied. Many puzzling effects, especially new types of phase transitions were found, calling for new models to capture these findings. Although the models are simple in definition, usually exhibiting Ising spins coupled by nearest-neighbour interactions, their low-temperature behavior is still far from being fully understood. Since the numerical and analytical treatment of these models is very demanding, many new algorithms and techniques have been developed. These methods now have spread to many fields, especially interdisciplinary applications of statistical physics. Hence, it is fair to say that the study of spin glasses and random-field systems has influenced many areas of science and led to many new developments.

In this work, in particular the ferromagnet-paramagnet phase transition of the random-field Ising system is studied. All critical exponents are calculated independently for the first time by measuring several quantities and using exact ground-state algorithms. The findings are consistent with all (hyper-) scaling relations, but the behavior of the specific heat is different from the results found in experimental realizations, namely diluted antiferromagnets in a field.

Furthermore, several fundamental findings on the nature of the spin-glass phase, which has been subject of discussion for a long time, are presented. It turns out that at low temperatures the spin-glass phase is more complicated than predicted by the Droplet Scaling (DS) theory, but does not exhibit all properties of the replica symmetry breaking solution of the Sherrington-Kirkpatrick model.

Finally, the coverable-uncoverable transition of the vertex-cover problem on random graphs is studied. For small connectivities of the graphs, the phase boundary can be calculated exactly by mapping the model on a random magnetic system and by applying methods from statistical physics, in particular the Replica trick[1]. This is a major improvement over the upper and lower bounds found earlier by means of mathematical methods. The behavior of the full phase diagram, which has been obtained numerically, also for larger connectivities where the analytical ansatz fails, can be understood in terms of four percolation transitions occurring in the model. Finally, using the phase diagram obtained before, it is possible to calculate the typical running time of a Branch-and-Bound algorithm for solving the vertex-cover problem.

This work and its results would not have been possible without the support of many people. First of all, the author would like to thank Annette Zippelius. She hosted the author during three and a half years in Göttingen at the Institute for Theoretical Physics. The author benefited much from her support, in particular from her helpful advice, many fruitful discussions and from the scientific cooperation. The author also grateful to Peter Young and Werner Krauth, for their intense cooperations and for hosting him in Santa Cruz (USA) and Paris.

Furthermore he is very much obliged to Martin Weigt. The author enjoyed uncountable hours of a close cooperation consisting of invaluable discussions and many new ideas and findings in the field of complex systems. The author also benefited much from cooperations with Timo Aspelmeier, Wolfgang Barthel, Kurt Borderix, Martin Feix, Ulrich Geyer, Matthias Kölbel and Reiner Kree (Göttingen), Heiko Rieger (Saarbrücken), Michael Jünger, Frauke Liers and Dietrich Stauffer (Köln), Ulrich Nowak and Klaus Usadel (Duisburg), Dietrich Heermann (Heidelberg), Alan Bray, Adam Carter and Mike Moore (Manchester), Guy Hed and Eytan Domany (Rehovot), Alberto Rosso (Paris), Ian Campell (Montpellier), Helmut Katzgraber and Juan Moreno (Santa Cruz), Matteo Palassini (San Francisco), and Michele Leone, Federico Ricci-Tersenghi and Riccardo Zecchina (Trieste). Last, but not least, the author is indebted to all colleagues in Göttingen, Santa Cruz and Paris for the friendly working atmosphere. He would like to thank all of them very much!

[1]The analytical results were obtained by Martin Weigt, with whom the author has a close cooperation

This work was supported financially by the DFG (*Deutsche Forschungsgemeinschaft*) under grants Ha 3169/1-1 and Zi209/6-1 and by the *VolkswagenStiftung* within the program "Nachwuchsgruppen an Universitäten".

January 2004

Alexander K. Hartmann

Contents

1 Introduction

In contrast to phase transitions [1, 2, 3, 4, 5] in ordered systems, the critical behavior of systems with quenched and dynamically induced disorder is still not well understood. Many interesting phenomena in this field can be studied using simple discrete models, which can be simulated numerically very efficiently. Apart from contributing to the understanding of physics, many of these models have interdisciplinary applications, e.g. in biology, theoretical computer science or economy, hence progress in this field will have a large impact on other areas of science.

Within the scope of this text, the low-temperature behavior of random-field Ising systems, Ising spin glasses and combinatorial optimization problems originating in theoretical computer science are studied, mostly by use of numerical simulation methods, especially by ground-state calculations. Starting in the 80s of the last century there are growing relations between the fields of statistical physics and (theoretical) computer science. This is in particular true for the study of disordered glassy systems in physics and the research on optimization problems in computer science [6]. Both fields can benefit strongly from each other. In one way computer science helps physics: Recently developed efficient optimization algorithms [7] help to study the low-temperature behavior of physical models, like spin glasses, random-field systems or solid-on-solid models. The last decade has seen strong progress in simulation techniques, allowing to study problems which were previously out of reach. On the other hand, also developments in statistical physics have helped to develop or to improve existing optimization algorithms. The most prominent example is the invention of the simulated annealing method [8], which has been applied to a variety of optimization problems.

There is another way physics can help to contribute to computer science. Computational problems can be sorted into different classes. From the viewpoint of a person wanting to solve problems, a very convenient class is the class P. It contains the problems, which can be solved on a computer in a running time, which grows even in the worst case only polynomially with the size of the problem. These problems are called *easy*. But not all problems can be solved polynomially. There are problems, for which for sure no polynomial algorithm exists, e.g. the running time grows exponentially fast. These problems are called *hard*. Most of them have only academic applications. The most interesting problems lie on the interface between polynomial and exponential running time. They belong to the class of *nondeterministic polynomial* problems (NP) [9]. For a precise definition, see the section "Complexity Theory" in the appendix. The definition basically means that a *nondeterministic* computer can solve any problem from NP in polynomial time. Since a nondeterministic computer does not exist so far, the concept of NP is used mainly as a tool for analyzing and comparing problems.

Very important are *NP-complete* (NP-c) problem. An NP-c problem has the property that *all* problems from NP can be mapped onto it. Hence, an NP-c problem is as hard as any problem in NP. Interestingly, it appears that the NP-complete problems are hard as well, because no polynomial algorithm for any problem from NP-c has been found so far despite much effort. But there is no *proof* that the problems from NP-c are indeed hard. This is the so called *P-NP problem*, one of the great open questions in computer science[2]. Translating the P-NP problem in common speach, it means looking for an answer to the question "what is it that makes a problem hard?" Here statistical physics can help a lot. Using concepts from physics like the notion of phase transitions and by applying methods from statistical mechanics, many new results in this field can be obtained.

The main body of this text, following the introduction, consists of tree parts. In each part a certain model is studied. The emphasis is on introduction and on informations not given in the papers which are reprinted in the appendix. Furthermore, the most important results from these papers are stated.

The first two parts concern models for disordered magnetic systems. In the first part, the low-temperature behavior of random-field Ising magnets (RFIMs) is studied. The ground-state calculation for the RFIM is a polynomial problem, hence large system sizes can be studied. The main results obtained here are the critical exponents describing the ferromagnet-paramagnet transition of three- and four-dimensional systems. The second part is devoted to Ising spin-glasses. This problem belongs to both classes P and NP-c, because in two dimensions the problem is easy, while in three dimensions it seems hard. Here, for two-dimensional spin glasses, the scaling behavior of excitations is investigated. For three-dimensional spin glasses, the morphology of the low-energy landscape is studied, in particular the question whether it exhibits a signature of replica symmetry breaking.

In the third main part an NP-c problem from theoretical computer science is presented, the vertex-cover problem (VC). It lies on the borderline between easy and hard problems, since it exhibits an easy-hard phase transition when studied on an ensemble of random graphs. Using concepts and methods from statistical physics it is possible to learn more about VC than when using only traditional mathematical methods.

In the appendix a short introduction to complexity theory is given, serving as a basis for understanding and classifying the problems which are covered in this text. While the fundamentals of statistical physics can be assumed to be known here, the reader may be not familiar with the concepts of theoretical computer science.

[2]The Clay Mathematics Institute of Cambridge, Massachusetts (CMI) has designated a $1 million price for the solution of the P-NP problem.

2 Random-field systems

Random-field systems [10, 11, 12, 13] and spin glasses [14, 15, 16, 17] are two prototypical models with quenched disorder. The main constituents are localized magnetic spins with random interactions. This types of models exhibit almost all basic phenomena occurring in statistical physics of disordered systems, like complexity, glassiness and aging. The study of these systems, due to their behavior distinct from the behavior of ordered systems, has led to many theoretical and experimental advances in physics.

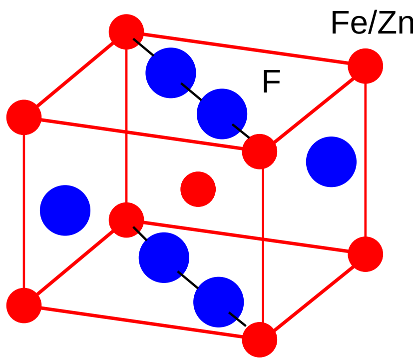

Figure 1: Crystal structure of $Fe_xZn_{1-x}F_2$. Small circles denote the Fe/Zn sites while the large circles are the F sites. The eight corner sites (Fe/Zn) are shared by 8 lattice cells, while the body-center site is not shared. The upper and lower pairs of F sites are shared by two cells, while the left and right sites are not shared. All together there are 2 Fe/Zn sites and 4 F sites per lattice cell.

Experimental realizations of random-field systems are *diluted antiferromagnets in a field* (DAFF) [18, 19]. One example is $Fe_xZn_{1-x}F_2$, where the variation of the local magnetic field on the Fe spins is caused by the varying concentration of Fe spins in the neighborhood due to the random replacement by non-magnetic Zn atoms, see Fig. 1 (The pure system Fe_xF_2 is an antiferromagnet). Experiments on this system [20, 21, 22] show a thermodynamic phase transition from an ordered low-temperature phase to a disordered high-temperature phase which is characterized by a logarithmic divergence of the specific heat, corresponding to the critical exponent[3] $\alpha = 0$, see Fig. 2. This phase transition is very different from ordered Ising systems, where $\alpha \approx 0.1$ has been found in three dimensions. One main subject of this work is to understand this behavior and to check whether it can be found in the behavior of simple models.

[3]Near a phase transition $T = T_c$, the behavior of the specific heat c can be described to first order by a $c \sim |T - T_c|^{-\alpha}$ behavior. In similar way, critical exponents for other quantities like the correlation legth ξ (exponent ν), magnetization m (exponent β) or susceptibility χ (exponent γ) can be defined.

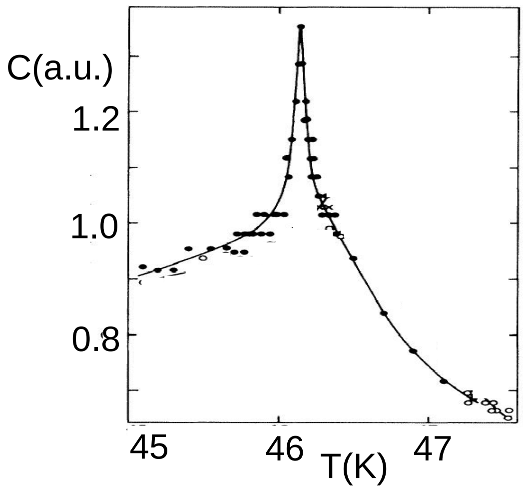

Figure 2: The specific heat of an diluted antiferomagnet measured experimentally [20].

The behavior of true diluted antiferromagnets agrees very well with computer simulations [23, 24, 25] of a simple corresponding Ising Hamiltonian. On the other hand, it is relatively hard to treat the model by means of an analytical approach [26]. As a consequence, random-field systems are usually studied instead, where the variation of the local magnetic fied is not induced by the neighbours, but put in directly.

For the most simple random-field model, classical Ising spins are located on the sites of a regular lattice, having pair or multi-spin interactions. Whereas spin glasses (see next section) are characterized by random interactions, random-field systems exhibit ferromagnetic interactions only. The randomness and complexity of the model is due to local random magnetic fields. Here d-dimensional hypercubic lattices of Ising spins $\sigma_i = \pm 1$ are considered. For the *random-field Ising magnet* (RFIM), each spin interacts ferromagnetically with its nearest neighbors. A local random magnetic field B_i acts on each spin. The system has the following Hamilton function

$$H = -\sum_{\langle i,j\rangle} J_{ij}\sigma_i\sigma_j - \sum_i B_i\sigma_i \tag{1}$$

The sum $\langle i,j\rangle$ runs over pairs of nearest neighbors. $J_{ij} > 0$ denotes the strength of the interaction. For the model studied in this text, $J_{ij} = J$ is constant. Here quenched disorder realizations of the local magnetic fields $\{B_i\}$ distributed according a Gaussian distribution with zero mean and width h are treated.

For a while it was thought [27, 28, 29] that the critical behavior of the d-dimensional RFIM is equal to that of the $d-2$ pure ferromagnet. Indeed one can show [30] at least that two-dimensional RFIM systems exhibit an ordered phase only at zero temperature. But this assumption would also imply that the $d=3$ RFIM exhibits no ordered phase. This is not true, as has been shown later

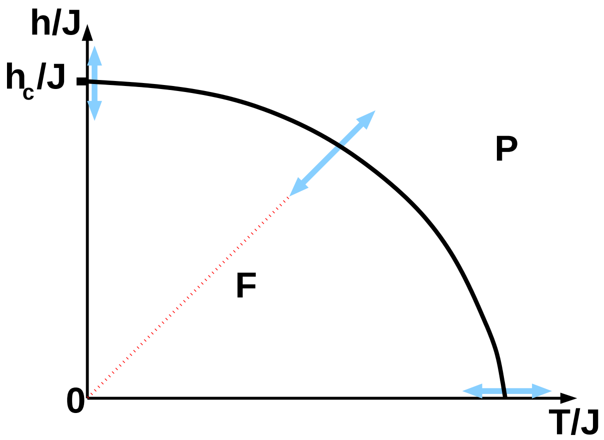

Figure 3: Phase diagram of RFIM with Gaussian distribution of the fields as obtained in mean field theory [43], the transition is 2nd order along the full line. F denotes the ferromagnetic phase, P the paramagnetic phase. For a bimodal distribution, there is a tricritical point on the line and the transition is 1st order above the tricritical point.

rigorously [31], i.e. in three or higher dimensions an ordered ferromagnetic phase exists for low temperatures and low strengths of the randomness. The phase diagram looks qualitatively like the mean-field phase diagram shown in Fig. 3. The transition between the ordered and the disordered phase is characterized by critical exponents, which quantify the critical behavior of quantities like correlation length, specific heat, magnetic susceptibility or magnetisation. For quite a while it was discussed [32, 33, 34, 35, 36, 37], whether for intermediate fields $h > h_c(T)$ there is an additional glassy phase, which is characterized by complex domains [38] and possibly by replica symmetry breaking. Corresponding results where found [23] in Monte Carlo (MC) simulations [39] of the dynamical behavior of the DAFF. On the other hand, recent numerical results for three dimensions [40, 41] give no evidence for a complex phase at intermediate disorder strength.

An analytic solution of the model was not possible so far for finite-dimensional systems. It has just been achieved for a mean-field model [42, 43], where every spin interacts with every other spin. For finite-dimensional systems a scaling theory [44, 45, 46, 47] for the RFIM was developed, where the dimension d has been replaced by $d - \theta$ in the hyper-scaling relations, θ (sometimes called also y) being a *third* independent exponent, in contrast to the pure case. An alternative approach [48, 49] leads to the consequence that θ is not independent but related to the exponent η describing the divergence of the (disconnected) susceptibility via $\theta = 2 - \eta$. For three-dimensional systems, computer simulations [50, 51] of small systems (up to $N = 16^3$ resp. $N = 32^3$ spins) have been performed to obtain the critical exponents. Surprisingly these exponent values do not fulfill some scaling relations, which have been derived before [44, 45, 46, 47]. Therefore, the question arises whether either the systems sizes of the simulation were too small or it was not possible to obtain thermal equilibrium.

Regarding the question of the values of the critical exponents, since the random-field fixed point is at $T = 0$ [45, 47], it can be assumed that the behavior at $T = 0$ can be found also for finite temperatures, at least near the fixed point. Thus the exponents for $T > 0$ can be obtained from classical ground-state calculations ($T = 0$) as well. As it will be explained below [52, 53, 54, 55, 56], the ground-state calculation for the RFIM belongs to the class P, which allows to treat much larger systems than it is possible with Monte Carlo simulations [39]. Furthermore, since the ground-state algorithms are exact, one encounters no problems to obtain equilibration.

Here, first the mapping of the RFIM to networks is outlined and it is explained that the ground-state energy corresponds to the maximum flow through the network. Furthermore it is described how the ground-state configuration can be obtained from the maximum flow. Then briefly the idea of an algorithm to obtain the maximum flow is presented. In second subsection, the results obtained from ground-state calculations for three- and four-dimensional random-field systems are summarized.

2.1 Ground-state calculation

For a given RFIM realization, an equivalent network can be constructed such that the maximum flow through the network is equal to the ground-state energy of the RFIM. This transformation was introduced by Picard and Ratliff in 1975 [52]. Here the transformation is just outlined, a detailed presentation can be found in Ref. [7].

In addition to the ground-state energy, the orientations of the spins in a ground state can be easily constructed from the flow values the network takes, see below. In the case where the ground state is degenerate, e.g. when a bimodal $\pm h$ distribution for the local fields is used, all ground states can be obtained by a subsequent calculation [57, 58, 59, 60] [4].

The algorithm is based on the notion of a network, which is a graph with additional capacities. Formaly, a network is a four-tupel $N = (G, c, s, t)$, where $G = (V, E)$ is a directed graph which has $n + 2$ vertices, $c : V \times V \to \mathcal{R}_0^+$ are the capacities of the edges $(i, j) \in E$, with $c(i, j) = 0$ if $(i, j) \notin E$. The vertices $s, t \in V$ are the *source* and the *sink* of the network, respectively. For convenience, we use $V = \{0, 1, \ldots, n, n + 1\}$ where $s \equiv 0$ and $t \equiv n + 1$, and the notation $c_{ij} \equiv c(i, j)$. The vertices in $V \setminus \{s, t\}$ are called *inner vertices*. Edges connecting only inner vertices are called *inner edges*.

[4]There are other systems, where the ground-state calculation can be mapped onto maximum-flow problems in networks. Examples are interfaces in random elastic media [61, 62] and fracture surfaces in random fuse networks [63].

A network can be interpreted as a system of streets connecting the source with the sink. The capacities c_{ij} tell how much flow (e.g. number of cars) can run through a given route per time unit. Now, assume that the network should be divided into two pieces in a way that the source and the sink are separated. You can think of the Austrian motorway system and a group of ecologists who like to prevent lorry drivers from taking the motorways to Italy[5]. Mathematically, this separation is a (s,t)-*cut* $(S,\overline{S})$ which has the following properties:

$$S \cup \overline{S} = V, \quad S \cap \overline{S} = \emptyset, \quad s \in S, \quad t \in \overline{S} \tag{2}$$

Usually, we denote the elements of S *left* and the elements of $\overline{S}$ *right* of the cut.

Since the amount of work (or the number of ecologists) to block a street grows with its capacity, the ecologists are interested in knowing the capacity of the streets they have to block. These are exactly the streets which go from S to $\overline{S}$, that means from left to right. We say these streets/edges *cross* the cut. Edges in the opposite direction cannot contribute additionally to a flow from the source to the sink, thus they are disregarded for the calculation of the capacity. The sum of the capacities of the contributing edges is called the *capacity* $C(S,\overline{S})$ of the cut:

$$C(S,\overline{S}) = \sum_{i\in S, j\in\overline{S}} c_{ij}\,. \tag{3}$$

By introducing a binary vector $\underline{X} = (x_0, x_1, \ldots, x_n, x_{n+1})$ with $x_i = 1$ if $i \in S$ and $x_i = 0$ if $i \in \overline{S}$ one can rewrite the capacity of a cut as a quadratic function over the x_i's. Using the fact that the source and the sink are fixed, i.e. $x_0 = 1$, $x_{n+1} = 0$, and by mapping the 0/1-variables on spin values, i.e. $x_i = 0.5(\sigma_i + 1)$ for $i = 1, \ldots, n$, one can obtain a one-to-one correspondance of the interaction constants $\{J_{ij}\}$ and the values of the random-fields $\{B_i\}$ to the capacities $\{c_{ij}\}$. The capacities of the inner edges are determined directly by the interaction constants via $c_{ij} = 4J_{ij}$ $(i > j)$, while the capacities of the other edges depend also on the random fields [7]. Then, every configuration of the system corresponds to a cut in the network via $\sigma_i = 2x_i - 1$ and the energy $H(\sigma_1, \ldots, \sigma_n)$ is equal to the capacity $C(x_1, \ldots, x_n)$ of the corresponding cut.

Since we are interested in ground states, a minimum of the energy is to be obtained. Consequently, we are looking for a *minimum cut*, that is a cut of minimum capacity. Such a cut cannot be obtained directly, but it is related to the flow going through the network in the following way. Each flow must pass the edges crossing an arbitrary cut, in particluar the minimum cut. Therefore, the minimum cut capacity is an upper bound for the flow. On the other hand, it can be shown that the maximum flow which is possible is indeed given by the capacity of a minimum cut. The proof was found by Ford and Fulkerson

[5] This happend in October 2002. It is not known whether Mathematicians were involved in optimizing the blockade.

in 1956 [66]. Versions of the proof which are more instructive can be found in [67, 68, 69]. Along with the proof, a simple method for finding the maximum flow was introduced. Hence, after constructing an equivalent network, such an maximum-flow algorithm can be applied to find a ground state of a random-field Ising system. The Ford-Fulkerson algorithm is outlined below.

Apart from calculating the ground-state energy, one can obtain also the corresponding ground-state configurations. *One* single minimum cut, which represents one spin configuration of minimum energy, can be found in the following way, which is a special variant of a breadth-first search: the basic idea is to start at the source and then to follow only edges where the flow is less than the capacity. Consequently, the spins visited are always on the left side of the minimum cut, since only edges which are satisfied can cross it. After all vertices have been visited, which are accessible from the source in this way, the iteration stops. Then the spins which have been visited are left of the cut, so they are set to orientation $+1$. The remaining spins are set to orientation -1.

In this way only one ground state can be obtained, even if the system is degenerate. A simple method to find *different* ground states in different runs of an algorithm has been presented in [58]. To actually find *all* different ground states one must find *all* existing minimum cuts. This can be achieved with a method explained in [57]. The result is a graph which describes all possible minimum cuts. Since the ground state is unique for a Gaussian distribution of the random fields, the simple method to obtain the ground state configuration is sufficient here.

Next, the basic idea of algorithms for calculating the maximum flow in a network is given. Mainly a description of the historically first method, which was invented by Ford and Fulkerson in 1956 [66], is presented here. Then it is outlined, how the extensions of the Ford-Fulkerson method work, which are used in modern algorithms.

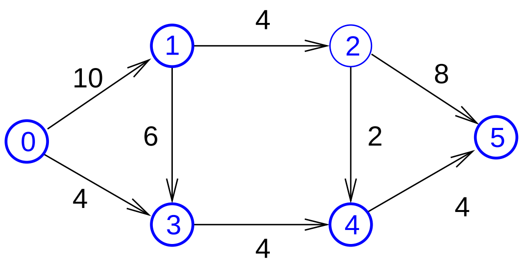

Figure 4: A small sample network. Vertex 0 is the source, vertex 5 the sink. The numbers close to the edges denote the edge capacities.

The basic idea of the Ford-Fulkerson algorithm is to start with an empty network, for an example see Fig. 4, and to try to push interatively (additional) flow from the source to the sink. This is done by searching for paths along

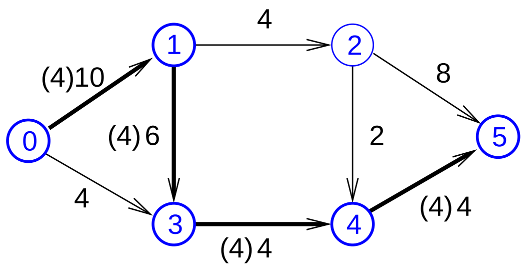

Figure 5: An augmenting path (bold edges) in the sample network. The numbers in brackets denote the flow values.

which the flow can be increased, they are called *augmenting paths*. A sample for an augmenting path is shown in Fig. 5. The amount of flow, which can be additionally pushed along the augmenting path, is determined by the minimum *residual capacity*, i.e. the minimum difference between capacity and current flow. Note that for each single edge, sometimes it may necessary to decrease the flow to increase the total flow. This case appears when a certain amount of flow is redirected within the graph, as shown in Fig. 6. If no augmenting path is found, the algorithm stops and the maximum flow has been found. [6]

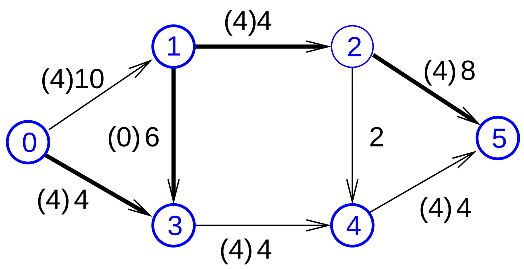

Figure 6: Another augmenting path (bold edges) in the sample network. Here the flow through the edge $(1, 3)$ is decreased to zero, hence the flow is redirected. No further flow increment is possible.

As mentioned, for each augmenting path the edge with the smallest residual capacity $r_{\min}$ is a bottleneck. This means the flow along the path can be increased only by $r_{\min}$, which slows down the computation. Even worse, the running time of the Ford-Fulkerson algorithm is *not* bounded by a polynomial in the number of nodes $N = |V|$. The reason is that an "unfortunate" choice of the augmenting paths might lead to many iterations where e.g. the flow is alternately increased through one path and then redirected through another path. An example is given in Ref. [7]. The running time of the Ford-Fulkerson algorithm is instead bounded

[6]The algorithm works for rational capacity values, i.e. it may not converge to the true maximum flow if the capacities are irrational, an example is given in Ref. [70].

by the capacity of the minimum cut, which itself is bounded by $|E|c_{\max}$, where $c_{\max}$ is the maximum occurring capacity.

This unfavorable behavior is avoided by an extension of the algorithm, which was presented by Edmonds and Karp in 1972 [71]. The basic idea is to choose an augmenting path which has the shortest distance from the source to the sink, where each edge counts with distance one[7]. It can be shown that indeed this algorithm has a polynomial worst-case time complexity of $\Theta(|V||E|^2)$, which is in fact independent of the capacities of the edges.

Modern algorithms are even faster. The basic idea is that the flow is not augmented through one path, but through *many* paths at the same time, as proposed by Dinic [72]. This concept is used in Tarjan's *wave-algorithm* [73] and in so called *push-relabel* algorithms [74, 75, 76]. The push-relabel method is implemented in the LEDA library [77], which is distributed commercially. For the RFIM it exhibits a running time, which grows like $O(N^{4/3})$ with the system size [59, 78], i.e. only slightly stronger than linearly with the number of spins. Using this modern algorithms, system sizes like $N = 100^3$ are feasible on typical workstations having 500MB of main memory.

2.2 Summary of results

First the results for the three-dimensional RFIM are presented. Included is also a brief description of the methods used here to measure the critical behavior of the specific heat and of the susceptibility. In the second part, the results for four-dimensional systems are given.

As already mentioned, the critical exponents of the ferromagnet-paramagnet transition line can be obtained from ground-state calculations. This works by calculating ground states for several values h of the random-field strength and performing an average over the realizations, denoted by $[\ldots]_h$. Here, for three dimensions, ground states for systems having sizes up to $N = 96^3$ with a Gaussian distribution of the local fields were obtained. Each realization is characterized by a set $\{\epsilon_i\}$ of random variables taken from a Gaussian distribution with zero mean and unit width, the random fields are $h_i = h\epsilon_i$.

In a previous work [79] already the average absolute magnetisation $m = \frac{1}{N}[|\sum_i \sigma_i|]_h$ and the disconnected susceptibility $\chi_d = \frac{1}{N}[(\sum_i \sigma_i)^2]$ for different sizes were measured. A critical field of $h_c = 2.28(1)$ was found. By applying a finite-size scaling analysis, the corresponding critical exponents $\beta = 0.02(1)$ for the magnetisation, $\overline{\gamma} = 3.5(5)$ for the disconnected susceptibility and $\nu = 1.19(8)$ for the correlation length were obtained. Similar results were found previously for smaller sizes using Monte Carlo simulations [50, 51], smaller resp. similar

[7]Another version of the algorithm always chooses the augmenting path with the maximum increment $r_{\min}$. This results in a time complexity of $\Theta(|E| \log c_{\max})$, where $c_{\max}$ is the maximum capacity of all edges.

sizes (but only for ν in the latter case) using again ground-state calculations [53, 80, 81, 82] and later for ground state calculations of larger systems [41].

The aim of this work [A, B] is to determine all critical exponents independently, without using (hyper-)scaling relations, hence the critical exponents for the specific heat and for the susceptibility remain to be obtained.

In zero random field, the specific-heat exponent is obtained from the singularity in the second derivative of the free energy with respect to temperature. More generally it is determined from the singularity obtained by varying a parameter which crosses the phase boundary from the paramagnetic phase to the ferromagnetic phase. From Fig. 3 we see that this can be conveniently accomplished by keeping the ratio of h/J to T/J fixed, i.e. by varying J. The first derivative of the free energy (per spin) F with respect to J, called here the "bond energy" E_J, is given by

$$E_J \equiv \frac{\partial F}{\partial J} = -\frac{1}{N} \sum_{\langle i,j \rangle} \langle \sigma_i \sigma_j \rangle, \tag{4}$$

where $\langle \cdots \rangle$ is a thermal average, and the sum is over nearest-neighbor pairs. E_J has an energy-like singularity in the vicinity of the phase boundary.

Derivatives of E_J cannot be calculated analytically, hence a first-order finite difference was applied to determine the derivative of E_J numerically. Since this is a more accurate representation of the derivative at the midpoint of the interval than at either endpoint, the "specific heat", C, at $T = 0$ is defined to be

$$C\left(\frac{h_1 + h_2}{2}\right) = \frac{[E_J(h_1)]_h - [E_J(h_2)]_h}{h_1 - h_2}, \tag{5}$$

where h_1 and h_2 are two "close-by" values of h. I.e. here the derivative $\frac{\partial^2 F}{\partial J \partial h}$ is considered. It can be shown [A] that all second derivatives invovling J and h exhibit the same critical behavior. A similar approach has been used in Ref. [83], but there the actual data was recorded within a Monte Carlo simulation [39] and for smaller systems (up to $L = 20$).

From a finite-size scaling analysis, one finds [A] that the specific heat does not diverge, even not logarithmically, but that it converges to a finite value in the thermodynamic limit. This means the specific heat exhibits a cusp. The finite-size dependence of the maximum is given by $C^{\max}(L) = C_\infty + a_2 L^{\tilde{\alpha}/\nu}$ with $\tilde{\alpha}/\nu = -0.48(3)$. For use in scaling relations, one has to realize that the dominating part (i.e. usually the diverging part) determines the critical exponent. Hence, in this case, where the approach is to a nonzero constant, this is described by the critical exponent $\alpha = 0$. This is compatible with the results in Ref. [41]. But in Ref. [41] the specific heat was not determined directly. Scaling relations for E_J and the energy of domain walls were used instead, hence it was not possible to distinguish between a logarithmic divergence and a convergence to a finite value, which are both described by the exponent $\alpha = 0$. In experiments with diluted antiferromagnets a logarithmic divergence is found. This means that the assumption that DAFF and RFIM are equivalent might not be true. We expect that ground-state calculations for the DAFF, which are possible exactly in polynomial time as well, will clarify this question.[8]

The susceptibility can be obtained by considering the response to a small uniform external field H, i.e. one considers the Hamiltonian

$$\mathcal{H} = -J \sum_{\langle i,j \rangle} \sigma_i \sigma_j - \sum_i h_i \sigma_i - H \sum_i \sigma_i \,. \qquad (6)$$

For each given realization and value of h, one calculates the magnetisation for few different small values of H, for details see Ref. [A]. Near $H = 0$, the data points can be fitted very well with a parabola, the coefficient of the linear term gives the zero field susceptibility $\chi = dm/dH|_{H=0}$.

From a finite-size scaling analysis, an algebraic divergence of the susceptibility near the phase transition $h_c = 2.28(1)$ was obtained, described by the critical exponent $\gamma/\nu = 0.50(3)$. This is compatible with results from Monte Carlo simulations [50, 51] and series expansions [84, 85].

Since the values of the critical exponents are determined independently, different (hyper-) scaling relations [3] can be tested. Indeed all scaling relations, e.g. $\alpha + 2\beta + \gamma = 2$ or $(d - \gamma/\nu)\nu = 2 - \alpha$ are fulfilled for the values given above, nevertheless the difference to experiments (logarithmic or no divergence of the specific heat) remains to be clarified.

For four-dimensional systems a similar study [B] was carried out. Exact ground states for systems up to size 32^4 were obtained. Again, the magnetisation, the disconnected susceptibility, the susceptibility and the specific heat-like quantity and in addition the Binder cumulant [86, 87] of the magnetisation are calculated. Using finite-size scaling techniques, the corresponding critical exponents are obtained: $\beta = 0.13(5)$, $\overline{\gamma} = 2.83(50)$, $\gamma = 1.42(20)$. For the specific heat both $\alpha = 0$ (logarithmic divergence) and an algebraic divergence with $\alpha = 0.26(5)$ are compatible with the data. Furthermore, values for the critical randomness $h_c = 4.18(1)$ and the correlation-length exponent $\nu = 0.78(10)$ were found. These independently obtained exponents are compatible with all (hyper-) scaling relations. Compatible results were found previously from ground-state calculations of smaller sizes $(h_c, \nu, \beta, \bar{\gamma})$ [81] and later of larger sizes (all except γ; a higher preference for an algebraic divergence of the "specific heat") [88] and from a series expansion yielding $(\gamma, \overline{\gamma})$ [84, 85].

[8] For the DAFF additional problems arise, because the averaged bond energy E_J is not a continuously differentiable function, hence additional methods for the data analysis have to be developed.

3 Spin glasses

Similar to the RFIM, which was covered in Chap. 2, a spin glass is a disordered system having localized spins. Spin glasses have a more complex behavior than random-field systems. Spin glasses exhibit ordered phases, but without spatial order of the orientations of the spins due to the existence of competing interactions. From the computational point of view, spin glasses are very interesting as well, because the ground-state calculation is NP-complete. For these and other reasons, spin glasses have been among the central topics of research in material science and statistical physics during the last three decades. Many analytical approaches in statistical physics and many optimization methods invented so far have been applied to spin glasses. Introductions to spin glasses can be found in Refs. [14, 15, 16, 17]. Recent developments are covered in Ref. [13].

A spin glass can be created using well known materials [17], e.g. one takes a lattice of a non-magnetic conducting material like gold and replaces a small fraction x of gold randomly by magnetic iron ($\mathrm{Fe}_x\mathrm{Au}_{1-x}$). To see the spin glass behavior in an experiment, the system is subjected to a weak magnetic field and cooled to a low temperature. Then the resulting magnetisation is measured, i.e. one obtains the magnetic susceptibility χ. When studying χ as a function of temperature T one observes a peak at a very low temperature T_G [96]. Usually T_G is of the order of 10 Kelvin, the exact value depends on the concentration x of the iron and on the way the sample is prepared. This peak is an indication for a phase transition. But when measuring the specific heat $C(T)$, a smooth behavior around T_G is found, only a broad maximum usually at higher temperatures can be observed. This is in strong contrast to usual phase transitions. Furthermore, when performing a neutron-scattering experiment, one finds that below the transition temperature T_G, spin glasses exhibit no spatial (e.g. ferro- or antiferromagnetic) order of the orientation of the spins.

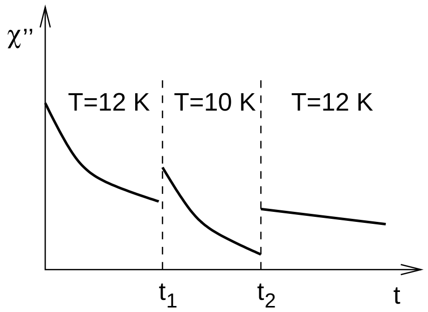

Figure 7: Aging experiment. A system is cooled down to $T = 12\,\mathrm{K}$, then the dynamic susceptibility is measured for a while. After time t_1 the system is suddenly quenched down to $10\,\mathrm{K}$, again the susceptibility is measured. After a while the system is heated back to $12\,\mathrm{K}$. At time $t_1 + t_2$ the system remembers the state it had at time t_1.

Even more puzzling are *aging* experiments, where spin glasses are examined with respect to the time evolution and the history of the system. A sample experiment is shown in Fig. 7. A spin glass is first cooled to $T = 12\,\mathrm{K}$ and kept there for a while [97]. The imaginary part χ'' of the dynamic susceptibility, describing the response of the magnetisation to a weak applied alternating field (here with $\omega/2\pi = 0.01\mathrm{Hz}$), is measured as a function of the time. After time t_1 the system is quenched to 10 K, a jump of the susceptibility occurs. Again the system evolves for a while. After time t_2 the system is heated back to 12 K. Now the susceptibility switches back to the value it had a time t_1. Hence, the system has remembered its state it had at temperature 12 K (*memory effect*). Such types of experiments are not understood so far in detail, only heuristic explanations exist. This is one reason why spin glasses have attracted so much attention in the past and will probably also attract it in the future.

The basic reason for this strange behavior is the type of interactions which can be found in this class of materials. The behavior of the Fe_xAu_{1-x} alloy is governed by the indirect-exchange interaction, usually called *RKKY* (Ruderman, Kittel, Kasuya, Yosida) interaction. The main point is that the sign of the interaction changes with distance. In the iron-gold alloy, since the iron is place randomly in the gold host, each spin interacts with some spins ferromagnetically and with others antiferromagnetically, causing the complex spin-glass behavior. There are other ways of creating interactions with different signs: some types of systems exhibit super exchange or other dipolar interactions. There are also different mechanisms creating disorder: in the case of Fe_xAu_{1-x} the randomness is obtained by placing the iron atoms at random chosen sites of a lattice. Also amorphous metallic alloys like $GdAl_2$ and YFe_2 show spin-glass behavior. For another class of systems, the lattice sites are occupied in a regular way, but the sign and the strength of the bonds are random, in the spirit of a simple the Hamiltonian given below. Examples of such *random-bond* systems are $Rb_2Cu_{1-x}Co_xF_4$ and $Fe_{1-x}Mn_xTiO_3$. All together, this leads to a huge number of materials showing spin-glass behavior at low temperatures, more details can be found in [17].

A suitable theoretical model describing spin glasses is similar to the RFIM model (see Chap. 2), but it comprises bond randomness as a key element. Again, it is sufficient to concentrate on Ising spins $\sigma_i = \pm 1$ to find the main spin-glass properties. N spins are placed on the sites of a regular lattice with linear extension L, e.g. a quadratic ($N = L^2$) or a cubic ($N = L^3$) lattice. The spins interact ferromagnetically or antiferromagnetically with their nearest neighbors. A small example is shown in Fig. 8. The Hamiltonian is given by

$$H \equiv - \sum_{\langle i,j \rangle} J_{ij} \sigma_i \sigma_j . \tag{7}$$

The sum $\langle i, j\rangle$ runs over all pairs of nearest neighbors and J_{ij} denotes the strength of the bond connecting spins i and j. It is also possible to add a term describing

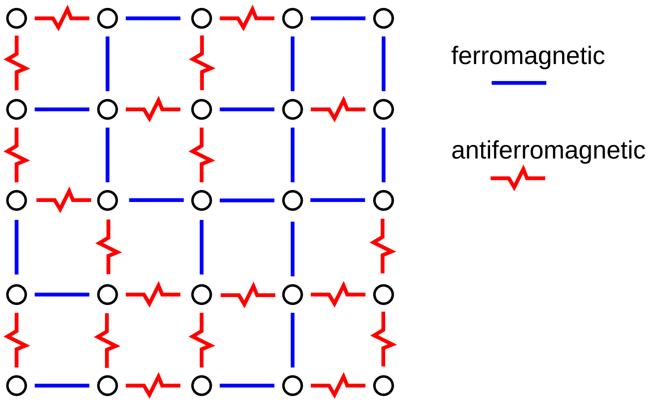

Figure 8: A two-dimensional spin glass with bond disorder. Spins are placed on the sites of a regular grid. They interact with their neighbors, the interaction is random, either ferromagnetic or antiferromagnetic.

the interaction with an external field B, but here we will concentrate on the case $B = 0$. This kind of model was introduced by Edwards and Anderson [89] in 1975, usually it is called the EA model. It has a broad range of applications. Models involving similar energy formulae have been developed e.g. for representing neural networks [90], social systems [91, 92, 93] or stock markets [94].

Like for the RFIM case, quenched disorder is considered here. For each realization of the disorder, the values J_{ij} of the bonds are drawn according to a given probability distribution. Very common are the Gaussian distribution and the bimodal $\pm J$ distribution, which have the following probability densities:

$$
\begin{aligned}
p_G(J) &= \frac{1}{\sqrt{2\pi}} \exp\left(-J^2/2\right) &(8)\\
p_{\pm J}(J) &= 0.5\delta(J-1) + 0.5\delta(J+1) &(9)
\end{aligned}
$$

The main ingredients constituting a spin glass are *mixed signs of interactions* and *disorder*. As a consequence, there are inevitably spins which cannot fulfill all constraints imposed by their neighbors and the connecting bonds, i.e. there will be some ferromagnetic bonds connecting antiparallel spins and antiferromagnetic bonds connecting parallel spins. One says, it is not possible to *satisfy* all bonds. This situation is called *frustration*, the concept was introduced in Ref. [95]. In Fig. 9 an example of a small frustrated system is shown.

The main properties of spin glasses are expected to be independent of the details of the interactions. Computer simulations of the EA model [12, 14] reproduce the main results found in experiments: a peak in susceptibility, a smooth behavior of the specific heat and frozen configurations of the spins. Recently, also the results of some aging experiments have been reproduced in simulations

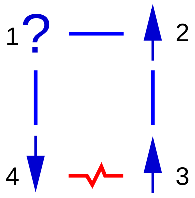

Figure 9: A frustrated plaquette at lowest energy. No matter which orientation spin 1 chooses, one of the bonds connecting it to its neighbors is not satisfied. Bonds 2-3 and 3-4 are satisfied.

[98, 99, 100, 101]. Therefore, one can conclude that even the simple EA model incorporates the main properties constituting a spin glass.

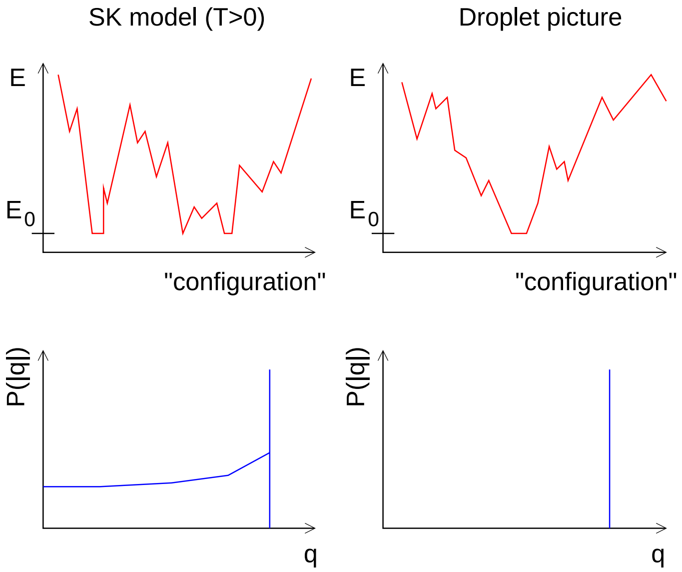

Figure 10: Mean-field solution vs. Droplet picture. The solution of the SK model exhibits a complicated energy landscape, resulting in a broad distribution $P(|q|)$ of the overlaps. In the Droplet picture, the system is dominated by only one pair of states at low temperatures, giving rise to a delta-distributed $P(|q|)$.

On the other hand, it is very hard to treat the EA model analytically [15, 16], even if one is interested just in the static behavior, on which is the concentration in this text. A mean-field (MF) version of the EA model was introduced by Sherrington and Kirkpatrick (SK) in 1975 [102]. It has been solved analytically for a Gaussian distribution of the interactions using the Replica trick and by introducing replica symmetry breaking (RSB) by Parisi in the 1980s [103]. The main property of the solution is that a complicated energy landscape is obtained (see upper left part of Fig. 10) and that the states are organized in a special hierarchical tree-like structure which is called *ultrametric*, for details see Ref. [104]. Furthermore, at low temperatures for typical realizations, there are always many configurations which are arbitrarily different. To measure the difference between two configurations $\{\sigma_i^\alpha\}, \{\sigma_i^\beta\}$, the *overlap* q can be used:

$$q^{\alpha\beta} \equiv \frac{1}{N} \sum_i \sigma_i^\alpha \sigma_i^\beta. \tag{10}$$

Thus, if $\{\sigma_i^\alpha\}$ and $\{\sigma_i^\beta\}$ are the same, we obtain $q = 1$, while $q = -1$ if the configurations are inverted relative to each other. If only about half of the spins have the same orientation, we get $q \approx 0$. Since a spin glass may exhibit many configurations with large thermodynamical weight even at low temperatures, one has to compare all of them pairwise. Each comparison results in an overlap value, so we end up with a *distribution of overlaps* $P_J(q)$. After averaging over the disorder an average distribution is obtained, denoted by $P(q)$. Due to the spin-flip symmetry of the Hamiltonian Eq. (7) usually $P(|q|)$ contains the full information. The result for the SK model at low temperatures is shown in the lower left part of Fig. 10. It exhibits a large peak called self overlap, which results from the overlaps of states belonging to the same valley in the energy landscape. Furthermore, within RSB, there are excitations containing $O(N)$ spins, i.e. of order system size, but having only energy $O(1)$, i.e. the energy is independent of the system size. This leads for $T > 0$ to a long tail down to $q = 0$ resulting from pairs of states belonging to different valleys.

Although the solution of the SK model is very elegant, it is restricted to this special spin-glass model. The question concerning the behavior of realistic, i.e. three-dimensional spin glasses is currently unsolved. One part of the physics community believes that also for three-dimensional systems a similar hierarchical organization of the states can be found, as in the SK model. Another group favours a description, the *Droplet* picture [105, 106, 107, 108, 109], which predicts a much simpler behavior. In that framework it is assumed that the low-temperature behavior is governed by basically *one* class of similar configurations (and their inverses), i.e. the energy landscape is dominated by one large valley, see right half of Fig. 10. Excitations involving $O(N)$ spins have an energy of order $O(L^{\theta_D})$ with $\theta_D \approx 0.19$ estimated from the scaling of domain-wall energies [110, 111, 112]. The main signature of this behavior is that the distribution of overlaps is a delta function in the thermodynamic limit $N \to \infty$. Recently, many results have been made available addressing this question, especially with numerical techniques [113, 114, 115, 116, 117, 118, 119, 120, 121], see also Sec. 3.4. Unfortunately the systems are very difficult to equilibrate near the transition temperature T_G, hence one is restricted to small system sizes. Even lower temperatures are not accessible using Monte Carlo methods [39]. As a consequence, a definite answer has not yet been obtained.

Furthermore, many numerical results exhibit properties of both mean-field and Droplet pictures. This has led to the development of additional scenarios aiming at the description of realistic spin glasses, for recent reviews see Refs. [122, 123]. For the other scenarios, one considers additionally the question, whether the interfaces separating different states are space filling or whether they have zero density in the thermodynamic limit. For this purpose one can measure the link-overlap

$$q_l^{\alpha\beta} \equiv \frac{1}{N} \sum_{\langle i,j \rangle} \sigma_i^\alpha \sigma_j^\alpha \sigma_i^\beta \sigma_j^\beta. \tag{11}$$

In RSB, the low-temperature excitations are space filling [124], this means that the distribution of link-overlaps converges to a non-trivial function in the thermodynamical limit as well. On the other hand for the Droplet picture, the surfaces of the excitations have zero density, i.e. the distribution of link-overlaps converges to a delta function.

This allows for two additional scenarios: In the *chaotic-pair* picture [125, 51, 127, 128, 129, 130], typical low-temperature excitations in finite systems are space filling but their energy grows like $O(L_D^\theta)$, hence in the thermodynamical limit the behavior is again governed by one large valleys (and its inverse). In the "TNT" ("trivial-non-trivial") scenario [116, 117] there are system-size excitations with energy $O(1)$, i.e. the distribution of overlaps is non-trivial, but they are not space filling, i.e. the distribution of link overlaps is trivial. The results presented in Sec. 3.4 are compatible with the TNT scenario, while recent Monte Carlo simulations [131] claim full RSB. Although there are no other scenarios which seem plausible in the moment, still fundamental notions are not fully clear. So it might be that the usual way of taking the thermodynamic limit is not valid for disordered systems [123]. Many new analytic tools have to be developed in the future for a better description of the behavior of spin glasses.

Before considering the three-dimensional case, we turn to two dimensions. Most results indicate that there is no spin-glass phase for finite temperatures, hence the simple Droplet scenario can be expected to be valid. In the next subsection, first an algorithm to calculate ground states for two-dimensional spin glasses is explained. Then the results for 2d are given. In the third subsection algorithms for 3d spin glasses are reviewed. In the last subsection the results for 3d are presented.

3.1 Algorithms for two dimensions

Although the ground-state problem for general spin glasses is NP-complete [132], for the special case of two-dimensional spin glasses without external field and with periodic boundary conditions in at most one direction[9], efficient polynomial algorithms [133] for the calculation of exact ground states are available. If

[9]This means the corresponding graph of interactions is planar.

one is interested in obtaining the partition sum, without obtaining spin configurations, one can also treat systems with full periodic boundary conditions in polynomial time, by using transfer-matrix approaches [134, 135, 136, 137, 137], but the running time is again strongly increasing, limiting the investigations to small systems. The most recent applications are based on matching algorithms [139, 140, 141, 142, 143, 144, 145, 146, 147], other exact approaches can be found in Refs. [148, 149]. Recently results for systems of size 1800×1800 were obtained [150].

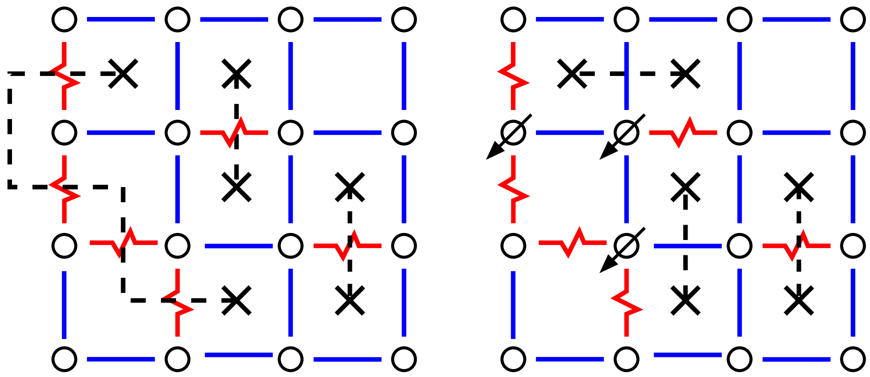

Figure 11: 2d spin glass with all spins up (left, up spins are indicated by empty circles). Straight lines are ferromagnetic, jagged lines antiferromagnetic bonds. The dotted lines connect frustrated plaquettes (crosses). The bonds crossed by the dotted lines are unsatisfied. In the right part the ground state with three spins pointing down (all other up), corresponding to a minimum number of unsatisfied bonds, is shown,

Here, just the basic idea of the algorithm is explained. For details, see Ref. [133, 151, 152]. The method works for spin glasses which are defined on planar graphs. In the left part of Fig. 11 a small 2d system with open boundary conditions is shown. All spins are assumed to be "up", hence all antiferromagnetic bonds are not satisfied. If one draws a dotted line perpendicular through all unsatisfied bonds, one ends up with the situation shown in the figure: all dotted lines start or end at frustrated plaquettes and each frustrated plaquette is connected to exactly one other frustrated plaquette, one says each pair of plaquettes is *matched*. Now, one can consider the frustrated plaquettes as the vertices and all possible pairs of connections as the edges of a (dual) graph. The dotted lines are selected from the edges connecting the vertices and called a *perfect* matching, since *all* plaquettes are matched. One can assign weights to the edges in the dual graph: they are equal the sum of the absolute values of the bonds crossed by the dotted lines. The weight Λ of the matching is the sum of the weights of the edges contained in the matching. Since Λ measures the total strength of the broken bonds, the energy of the configuration is given by $E = -\sum_{\langle i,j \rangle} |J_{ij}| + 2\Lambda$. This holds for *any* configuration of the spins, always a corresponding matching exists.

Obtaining a ground state means to minimize the total weight of the broken bonds (see right panel of Fig. 11), hence one is looking for a *minimum-weight perfect matching*. This problem is in the class P. Algorithms for minimum-weight perfect matchings [153, 154] are among the most complicated algorithms for polynomial problems. Here again the LEDA library offers a very efficient implementation [77], except that it consumes a lot of memory, which limits the size of the systems to about $N = 500^2$ on a typical 500 MB workstation.

For system with periodic boundary conditions in both directions, the matching approach is not feasible. In this case general purpose algorithms can be used, which are described in section 3.3.

To study the behavior of two-dimensional spin glasses, here not only ground states, but also low-lying excited states are generated. For this purpose ground-state algorithms can be used as well. The general procedure consists of these three steps:

1. Calculate ground state $\{\sigma_i^{(0)}\}$ of given realization, the ground-state energy is denoted by E_0.

2. Modify some (or all) couplings in a way that the ground state is penalized.

3. Calculate ground state of the modified system, which is usually a low lying excited state of the original realization. The new ground-state energy is E_0^m.

In this work three different ways of generating excitations are considered, for technical details, please refer to the reprints as cited.

- Domain walls are generated by changing the boundary conditions in one direction, e.g. from periodic to antiperiodic ("**P-AP**") or from free to fixed ("**F-DW**"), see reprints [C, D].

- Droplets are generated by changing all bonds slightly against the relative orientation of the original ground state. This is achieved by adding $\epsilon\frac{1}{N_b}\sum_{\langle i,j\rangle}\sigma_i^{(0)}\sigma_j^{(0)}\sigma_i\sigma_j$ to the Hamiltonian, see [E]. Therefore, the overall energy change of $\{\sigma_i^{(0)}\}$ is a constant ϵ and a different configuration may become ground state of the modified system (if ϵ is large enough).

- In Monte Carlo simulations, one can easily generate droplets, by fixing the boundary spins in the direction of the ground state and one (central) spin opposite to the ground state, i.e. by applying strong local fields. This is not possible for the matching algorithm, since it cannot handle magnetic fields. Nevertheless, when using a special scheme of changing the bonds and iterating over several modified systems, it is possible to generate droplets which are very similar to the single-spin-flipped droplets, see [F].

3.2 Results for two dimensions

For two dimensions, it is now widely accepted that there is no stable spin-glass phase for non-zero temperatures, i.e. $T_c = 0$ and $d = 2$ is below or at the lower critical dimension d_c. This issue can be studied by analysing the domain-wall energy $\Delta E = [|E_0^m - E_0|]_J$, where E_0 respectively E_0^m denote the ground-state energies of the unperturbed respectively modified system (see above) and $[\ldots]_J$ denotes the average over the disorder. For a Gaussian distribution of the disorder, one finds that ΔE decreases algebraically like $\Delta E \sim L^\theta$ $(\theta < 0)$ with system size [110, 155, 187], corresponding to a decreasing coupling strength when performing a real-space renormalization procedure of larger and larger blocks.

For a $\pm J$ distribution, the situation was less clear. Kawashima and Rieger [144] performed ground-state and domain-wall calculations for small systems ($N \leq 30^2$) and concluded $T_c = 0$. On the other hand, from Monte Carlo simulations [156] on sizes $N \leq 18^2$, it was claimed that $T_c > 0$. A calculation of domain-wall energies using a cluster MC method [157] for sizes $N \leq 24^2$ indicated marginal behavior (i.e. $d_c = 2$), and this was interpreted as evidence for a finite-T transition. Recently, Houdayer [158] used a more efficient cluster MC algorithm, which allows to treat larger systems ($N \leq 100^2$) to be studied down to low a temperature of $T = 0.1$. Houdayer finds that $T_c = 0$ but with an exponential divergence of the correlation length for $T \to 0$, which is consistent with $d_c = 2$, in agreement with earlier work by Saul and Kardar [134, 135]. On the other hand, for 2d systems with additional next-nearest neighbour interactions, there are indications [159] that indeed $T_c > 0$.

To clarify this situation, we have calculated [C] domain-wall energies via the exact ground-state algorithm using the procedure explained above. This allows to treat much larger system sizes than studied before, here up to $N = 480^2$. Also, one has no problems of equilibration, like one encounters when using Monte Carlo techniques.

For the $\pm J$ distribution, we have found for small systems a decrease of ΔE, but for larger systems, ΔE saturates at a non-zero value. This indicates that in this case the model is *right at* the lower critical dimension, i.e. $d_c = 2$. This is also compatible with recent results of Amoruso et al. [160], who have found a saturation of the domain-wall energy for all distributions where the possible domain-wall energies are not continuous, i.e. where they form a discrete set of values.

For a Gaussian distribution of the disorder, we have found a power law like in previous studies of small systems. But the value of the stiffness exponent θ turned out to depend slightly on the choice of the boundary conditions. For periodic boundary conditions in the x direction (P-AP case), we have found $\theta = -0.282(2)$. On the other hand for free boundaries in x direction (F-DW), we have found $\theta = -0.266(2)$. Both results are compatible with results found earlier [110, 155, 187], but are clearly incompatible with the assumption of universality, i.e. with the expectation that characteristic exponents do not depend on details of the model.

For this reason, we have applied [D] the aspect-ratio approach [161]. The basic idea is to study systems which have the size $N = L \times M$, where L respectively M measure the system extension in x respectively y-direction (the domain wall runs in the y direction). For $L \gg M$, i.e. for large aspect ratios $R = L/M$, the domain wall is in the x-direction far away from the boundary and should be independent of the choice of the boundary conditions. More precisely, a scaling form

$$\langle \Delta E \rangle = M^{\theta} F(L/M) \tag{12}$$

has been predicted [161], with the following limiting forms:

$$F(R) \sim \begin{cases} R^{-1} & & \text{for } R \to \infty \\ R^{\theta-(d-1)/2} & \text{(P-AP)} & \text{for } R \to 0 \\ R^{\theta-(d-1)} & \text{(F-DW)} & \text{for } R \to 0. \end{cases}$$

For a Gaussian distribution of the interactions, we have studied systems with aspect ratios $R \in [1/8, 64]$. The data turned out to fulfill the above given scaling form. Furthermore, the final resulting exponent $\theta = -0.287(4)$ is independent of the choice of the boundary conditions, i.e. universality holds. The reason for the deviation found before [C] is that due to the larger system surface the F-DW boundary conditions are more susceptible to finite-size corrections, hence larger systems are needed to see the behavior of the thermodynamical limit.

We have also found that the aspect-ratio approach does *not* work for the $\pm J$ case. The reason is that for large aspect ratios $R \gg 1$ the probability to find a domain-wall having non-zero energy decreases exponentially with R. For $R > 4$ and all practical number of realizations ($\sim 10^5$), the obtained average is exactly 0, independently of the size M. Thus, a scaling analysis is not possible.

Having determined the domain-wall energy exponent θ precisely, it is now instructive to check a prediction of the Droplet picture. It says that θ is equal to the exponent θ_D (often also just called θ) describing the scaling of the droplet energies with droplet resp. system size. Recently $\theta_D = -0.47 \neq \theta$ was determined for small systems using Monte Carlo simulations [162, 163, 164] and by studying lowest lying excitations [165]. For the Monte Carlo simulations first (heuristic) ground states where calculated, then a center spin was kept flipped with respect to the ground state while the border spins where kept fixed in the ground-state orientations, and a new ground state was calculated. For the work of Refs. [162, 163, 164] only systems of size up to $N = L^2 = 30^2$ were studied. We decided to mimic [F] this approach using matching algorithms. Since our approach involves the calculations of $2L$ ground states per realization, only system sizes up to $L = 160$ could be studied. The main quantity we have measured is the droplet energy as a function of system size. If one fits a pure algebraic decrease $L^{-\theta'}$ to the date for small systems $L \leq 30$ one indeed finds $\theta' = -0.45(1)$ compatible with the previous result [164]. Fitting the same function for large sizes $L \geq 80$ yields $\theta' = -0.32$ much closer to $\theta = -0.287$. Hence, the apparently different exponent found in Ref. [164] is due to too small system sizes.

The full behavior of the droplet energy E as a function of system sizes exhibits the following scaling form:

$$E = AL^{\theta} + BL^{-\omega}. \tag{13}$$

The term $BL^{-\omega}$ is a scaling correction to the droplet energy and A and B are positive constants. For $\theta = -0.29$ we have fitted the other three parameters to the function (13) and obtained a correction exponent $\omega = 0.97(5)$ and a very good quality $Q = 0.81$ of the fit. Hence, all results are compatible with the Droplet picture which says that the scaling behavior in 2d spin glasses, i.e. of droplets and domain walls, is described by one single exponent. For a triangular graph without full periodic boundary conditions in all directions a similar crossover for the scaling of the surface size of the droplets has been observed [167].

Currently, we are studying also the first excitations like in Ref. [165] but for much larger system sizes. Again a crossover of the energy from small system behavior (up to $N \leq 12^2$) to a different scaling at larger sizes can be observed and the data becomes again compatible with the one-exponent scenario [168].

Interestingly, the droplet exponent depends on the way the droplets are generated. We have also considered the method were all bonds are changed by a contribution of order ϵ, see previous subsection. One can obtain θ_D by a slightly different scaling analysis, e.g. from the measured probability to generate a large droplet [E]. Here, we have also studied systems with periodic boundary conditions, to encourage large droplets relative to the system size (one does not have to fix the boundary, which repells the droplet surface).

In such a case the graph is not planer and the matching algorithm cannot be applied. Instead we have used the Cologne spin-glass server [169], which uses a Branch-and-Cut approach [170, 171]. In this case no crossover could be observed. We have obtained an exponent $\theta_D = 0.32(2)$ which is slightly larger than the value found within the other approaches, but not too far away.

Recently another method [172] to obtain droplets has been applied to two-dimensional spin glasses of intermediate size $N \leq 64^2$ [173] and again depending on the way the droplet was generated, in one case a crossover of the droplet exponent to a value close to $\theta = -0.287$ has been observed, in the other case not. Hence, an understanding of the conditions under which a crossover has to be taken into account is still missing but is seems that in all cases the $\theta = -0.287$ behavior is obtained for large systems sizes, compatible with the Droplet picture.

3.3 Algorithms for three dimensions

In three dimensions, the situation is less clear. In this case, the ground-state calculation for spin glasses is NP-complete [132] i.e. the known exact algorithms exhibit exponentially increasing running time. This means that only small systems can be studied. Several algorithms are available, for an overview see [7, 55, 174]. The simplest method works by enumerating all 2^N possible states and obviously has an exponentially increasing running time. Even a system size of 4^3 is too large. The basic idea of the so called *Branch-and-Bound* algorithm [175] is to exclude efficiently some parts of the state space where no low-lying states can be found, so that the complete low-energy landscape of systems of size 4^3 can be calculated [176, 177, 178, 179]. Also transfer-matrix techniques have been applied [180] for spin glasses with $N = 4^3$. To evaluate all ground states, similar algorithms have been applied to two-dimensional systems as well [181, 182, 183, 184, 185, 186].

A more sophisticated method called *Branch-and-Cut* [170, 171] works by rewriting the quadratic energy function as a linear function with an additional set of inequalities which must hold for all feasible solutions. Since not all inequalities are known a priori, the method iteratively solves the linear problem, looks for inequalities which are violated, and adds them to the set until the solution is found. Since the number of inequalities grows exponentially with the system size, the same holds for the computation time of the algorithm. Thus, for Branch-and-Cut systems up to 8^3 are feasible. Further applications of these method can be found in Refs. [187, 188].

Since finding ground states in three-dimensional systems is computationally very demanding, several heuristic methods have been applied. At the beginning, simulated annealing was very popular, recent results can be found in Refs. [189, 190]. Usually it is very difficult to obtain true ground states using this technique. A more sophisticated method is the multicanonical method [191], which is based on Monte Carlo simulations as well, but incorporates a reweighting scheme to speed up the simulation. Very low-lying states of some systems up to size 12^3 have been obtained [192, 193, 194, 113, 195]. Heuristics which are able to find low-energy states but not true ground states unless the systems are very small can be found in Refs. [196, 197, 198]. Another approach included the application of neural networks [199].

Usually with minor success several variants of genetic algorithms [200] have been applied [201, 202, 203, 204, 205, 206, 207]. In a similar approach the population of different configurations was replaced by a distribution describing the population [208]. At first sight these approaches seemed to be very promising, but it is not possible to prove whether a true ground state has been found. One has always to check carefully, whether it is possible to obtain states with slightly lower energy by applying more computational effort. A genetic approach [209, 210] which was designed especially for spin glasses has been more successful. Realizations up to size 10^3 with Gaussian distributions of the bonds have been studied recently [211, 212, 213], supporting the Droplet picture for spin glasses. A combination with a recursive renormalization method can be found in Ref. [214]. The basic idea is to divide the problem into subproblems of smaller size and treat the subproblems in the same way. The technique has been applied to finite-dimensional systems with Gaussian distribution of the bonds [215, 216], again up to size 10^3, but also to other combinatorial optimization problems like the traveling salesman problem.

The method applied here, the genetic cluster-exact approximation (CEA) is able to calculate true ground states [112] up to size 14^3. Please note that just obtaining true ground states is not sufficient to obtain the correct thermodynamical result, i.e. not all configurations with the same energy are sampled in a way that they contribute to physical quantities with the same weight. This occurs for genetic CEA [217, 218, 219] but also for other methods based on Monte Carlo simulations [220]. Hence special measures must taken to ensure the correct sampling, this is the major part of the algorithm outlined below. It can also be used [I] to sample small systems up to $N = 10^3$ for low temperatures $0 < T < 0.5T_c$ in equilibrium. Here, the method is described for the general case $T > 0$, i.e. also excited states are generated. The special case $T = 0$ is obtained by including only ground states. The technique to obtain an equilibrated low-temperature sample consists of four steps, see also Fig. 12.

1. **Generate configurations for ground states and the lowest levels of excitations**

   The method is based on the special genetic algorithm of Ref. [209] as well but also incorporates the cluster-exact approximation (CEA) [221] algorithm. CEA is an optimization method designed specifically for spin glasses, but it should be applicable to all problems where each element (here: spin) interacts with a small number of other elements. Its basic idea is to transform the spin glass in a way that the max-flow methods can be applied, which work only for systems exhibiting no frustrations (see Chap. 2).

   By applying CEA alone, one can reach configurations very close to the true ground states. To find indeed the true ground states, one has to combine CEA with the genetic algorithm. The basic idea of genetic algorithms is to have a pool ("population") of configurations ("individuals"), optimize all of them separately, choose a fraction of better ("fitter") ones and throw the rest away, and combine the better ones to form new configurations ("crossover"), for details see Refs. [112, 221]. With this approach true spin-glass ground-state configurations can be obtained.

2. **On each energy level: group configurations into clusters**

   The configurations are sorted into *clusters* by performing the ballistic-search algorithm [G], which extends the usual neighbor search of the Hoshen-Kopelman algorithm [223]. All configurations which are accessible via flipping of single spins having zero local field (called *free spins* in the following), i.e. without changing the energy E, are considered to be in the same cluster.

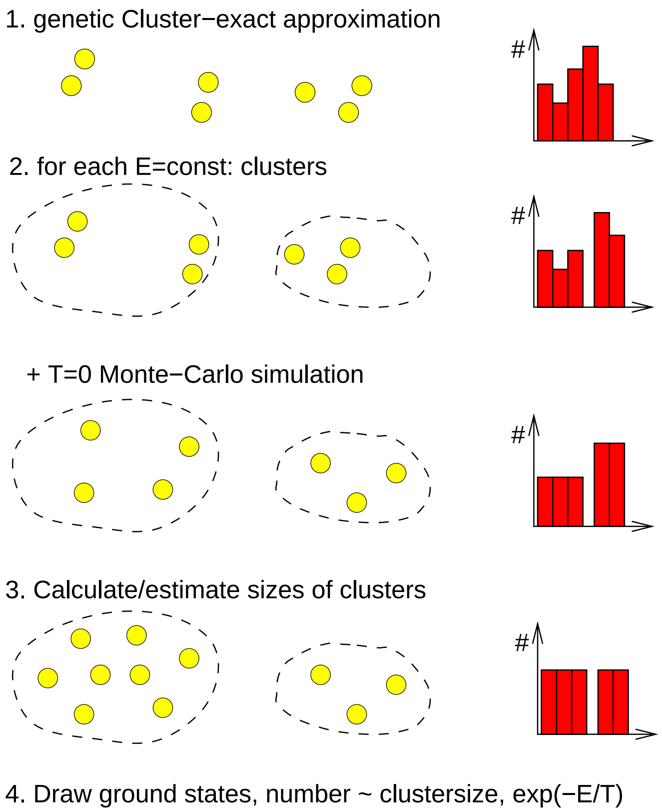

Figure 12: Summary of the algorithm to generate low-lying configurations at equilibrium. The histograms at the right show what happens to a statistics of the generated configurations all having the same energy, after each stage. At the end all configurations having the same energy occur with the same probability in a sample.

Please note that the Hamiltonian is symmetrical with respect to flipping all spins simultaneously. Hence, for the rest of the text and for all analysis steps, a configuration and its mirror image are regarded as being identical.

It cannot be guaranteed a priori that all clusters have been found by the initial calculation of the configurations. For small systems, where there are only few clusters, one can compare with exact enumerations [224]. For larger systems, one can increase the number of configurations included in the cluster analysis and monitor several quantities to establish the number of necessary configurations, for details see Refs. [H, I].

Furthermore, the configurations within each cluster, which are used for the further calculation, are obtained from a $T = 0$ Monte Carlo simulation of suitable length such that all configurations of a cluster contribute with the same weight/probability.

3. **Calculate sizes of clusters**

   Let $\mathcal{C}$ be a cluster we want to measure in size and let's consider a random 'reference configuration' $\{r_i\}$ belonging to this cluster. We define a test Hamiltonian $\tilde{H}[s] = -\sum_i r_i \sigma_i$ for $\{\sigma_i\} \in \mathcal{C}$, being $\tilde{E}(\beta)$ and $\tilde{S}(\beta)$ the average extensive energy and entropy at inverse temperature β. Then the size of $\mathcal{C}$ is given by $\exp[\tilde{S}(0)]$. Since the ground state of this Hamiltonian is unique (it is the reference configuration), i.e. $\tilde{S}(\infty) = 0$, we obtain from the micro-canonical definition of the temperature $T = d\tilde{E}/d\tilde{S}$

$$\begin{aligned} \tilde{S}(0) &= \tilde{S}(0) - \tilde{S}(\infty) = \Delta\tilde{S} = \int_{\tilde{E}(\infty)}^{\tilde{E}(0)} \beta \, d\tilde{E} = \\ &= \int_0^\infty [\tilde{E} - \tilde{E}(\infty)] \, d\beta = \int_0^\infty (\tilde{E} + N) \, d\beta \quad , \end{aligned} \tag{14}$$

   where the previous last equality comes from an integration by parts and the last equality from the substitution $\tilde{E}(\infty) = -N$. In order to calculate this integral, we actually perform a fast MC simulation restricted to configurations $\{\sigma_i\} \in \mathcal{C}$ while varying $w = \exp(-2\beta)$ in $[0,1]$ and measuring the average energy $\tilde{E}$ as a function of w. The final formula is the integral of a smooth function $\Delta\tilde{S} = \int_0^1 \frac{N+\tilde{E}}{2w} dw$.

4. **Generate a sample of states for given temperature** T

   Each cluster contributes with a weight proportional to its size and to the Gibbs-Boltzmann factor $\exp(-E/T)$, where E is the energy of the configurations in that cluster. The configurations are sampled in order of increasing cluster sizes, to ensure that also configurations from smaller clusters may contribute [H, I].

The composition of a cluster depends on the definition of what a cluster is. By choosing a dynamic which allows flips of more than one spin at a time, a different definition of energy-barriers is implied and thus another kind of clusters. It should be stressed that the results of the above algorithm *do not* depend on the way a cluster is defined. Any method of sorting the configuration into groups will work that takes the number of configurations selected proportional to the size of the group, and that ensures that each configuration of a group has the same probability of being used for the calculation.

As already indicated, the above presented algorithm to ensure an equilibrium sampling can be applied to the result of other simulation algorithms as well. Also for the results of Monte Carlo simulations, e.g. for simulated annealing [8] or parallel tempering [238, 239], it cannot be ensured a priori that all low-temperature states enter with the correct weight [220]. Finding ground states at all is much simpler than finding ground states having all the correct thermodynamic weight. Hence, by including the post-processing (steps 2-4), equilibrium sampling can be obtained for other methods as well.

3.4 Results for three dimensions

In three and higher dimensions, there is a stable spin-glass phase [13, 112, 225, 226]. There is a still ongoing controversy concerning the nature of this ordered phase, see the beginning of this chapter.

Since it is not possible to discriminate the different scenarios using analytical techniques, numerical methods have been applied. While earlier Monte Carlo simulations [87, 227, 229, 230] suffer from small system sizes or equilibration problems [231], recent results of simulations [232] at temperatures just below T_c seem to find evidence for the MF picture. In [233, 234], by applying a Migdal-Kadanoff approximation, which exhibits DS behavior automaticallyin the thermodynamic limit, MF-like behavior was found numerically for small systems at temperatures slightly below T_c, where the correlation length exceeds the system size. By going to lower temperatures or larger systems, DS behavior became visible again. Consequently, the analysis of true ground states should clarify the issue, because they dominate the behavior far away from the critical point. In Ref. [113] ground states were calculated using multicanonical MC sampling, but no discrimination between MF and DS could be made because of too small system sizes. In a recent work [211] evidence for the DS picture was found by calculating ground states of systems with Gaussian distribution of the interactions and applying several kinds of boundary conditions.

In this work, true ground states for the three-dimensional $\pm J$ model are calculated up to size $L = 14$ using the algorithm presented in the previous subsection, for technical details on the number of realizations etc. see reprint [H]. The distribution $P(|q|)$ of overlaps, see Eq. (10), is the main quantity to study the nature of the ground-state configuration space. To quantify whether $P(|q|)$ remains broad in the thermodynamic limit, the variance

$$\sigma^2(|q|) \equiv \int_{-1}^{1} (\overline{|q|} - |q|)^2 P(q) dq = \overline{|q|^2} - \overline{|q|}^2 \tag{15}$$

of the distribution and the weight

$$X_{q_0} \equiv \int_0^{q_0} P(|q|)\, dq \tag{16}$$

of the distribution below a given threshold q_0 are calculated. Since the mean $q_{\mathrm{EA}} = \langle |q| \rangle$ is $q_{\mathrm{EA}} = 0.90(1)$ [H], i.e. well above 0.5, $q_0 = 0.5$ was chosen.

Both quantities $\sigma^2(|q|)$ and X_{q_0} show a power-law L^κ decrease to zero. This means, in the thermodynamic limit, $P(|q|)$ is a delta-function, i.e. the ground-state landscape is trivial, similar to a ferromagnet. This does *not* imply that there are only two ground-state clusters remaining. On the contrary, the number of ground-state clusters grows exponentially with increasing system size [224] but the ground-state behavior is dominated by a few large similar clusters (and their inverses). Therefore, a distinct impression emerges: a huge number of arbitrarily different ground-state clusters exist, but by going to larger and larger sizes most of them become statistically unimportant. Interestingly, the result is compatible with the one step replica-symmetry-breaking scheme which was observed for the p-spin glass [242]. It exhibits a simple distribution of overlaps at $T = 0$ while many different ground-state clusters are possible.

Due to the numerical uncertainties, a convergence of e.g. X_{q_0} to a small but nonzero value is still possible. Indeed a reanalysis [236] of the data, by excluding trivial overlaps between configurations originating from the same ground-state clusters using a cluster analysis [237], shows that $P(|q|)$ might have a non-trivial tail of very small weight.

Hence, it is interesting, to further investigate the nature of the zero-temperature landscape. Here we also study whether the model exhibits *ultrametricity*, another characteristic of the MF solution. In an ultrametric space [104] the triangular inequality is replaced by a stronger one, which reads in terms of overlaps[10]

$$q^{\alpha\beta} \geq \min(q^{\alpha\gamma}, q^{\gamma\beta}) \ , \tag{17}$$

α, β, γ being three independent configurations. An example of an ultrametric space is given by the set of leaves of a binary tree, if the distance between two leaves is defined by depth of the closest commen ancestor.

Let $q_1 \leq q_2 \leq q_3$ be the overlaps $q^{\alpha\beta}$, $q^{\alpha\gamma}$, $q^{\gamma\beta}$ ordered according to their sizes. By writing the smallest overlap on the left side in (17), one realizes that two of the overlaps must be equal and the third may be larger or the same: $q_1 = q_2 \leq q_3$. Therefore, for the difference

$$\delta q \equiv q_2 - q_1 \tag{18}$$

$\delta q = 0$ holds. For a finite system, ultrametricity may be violated, i.e. $\delta q > 0$. If a system becomes more and more ultrametric with growing system size, δq should decrease while $L \to \infty$. When evaluating δq, the influence of the absolute size of the overlaps should be excluded. Thus, the third overlap is fixed: $q_3 = q_{fix}$. For an ultrametric system $P(\delta q)$ should converge to a Dirac delta function with increasing size L [235]. The numerical results are indeed compatible with a convergence to a delta function. It should be stressed that ultrametricity is only found for triplets of ground states with overlaps (here $q < q_3 \approx 0.5$) smaller than values from the dominating peak of $P(|q|)$. If indeed by performing the thermodynamic limit the weight of all regions of state space restricted in this way disappeared, then trivially ultrametricity would disappear as well.

By including excited states, the analysis of the low-temperature landscape was extended to finite temperatures, see reprint [I]. Due to the higher degeneracy of excited states, only system sizes up to $L = 10$ and $T = 0.5$, about half T_c, could be studied. For very small temperatures like $T = 0.1$ essentially the same states were sampled like for $T = 0$, at least for the system sizes studied here. For larger

[10] One can identify with an overlap $q^{\alpha\beta}$ the distance $d^{\alpha\beta} \equiv 0.5(1 - q^{\alpha\beta})$

temperatures $0.3 \leq T \leq 0.5$, excited states start to contribute to substancially the thermodynamic behavior. We have found that in this region clearly the distribution of overlaps becomes nontrivial, i.e. the width $\sigma^2(|q|)$ and the fraction $X_{0.5}$ of small overlaps converge to non-zero values in the thermodynamic limit. For larger sizes, excited states contribute also to the behavior at smaller temperatures, hence a similar behavior can be expected for all $T > 0$. Similar results have been found independently by Katzgraber, Palassini and Young [120, 121].

A non-trivial distribution of overlaps is not a sufficient criterion for a complex energy landscape. A qualitatively similar overlap distribution with a nonzero weight for small values of q would be obtained also for a system, where various configurations differ by a domain wall through the system at different positions, e.g. a ferromagnet with antiperiodic boundary conditions in one direction [240]. To rule out this scenario, we have calculated also the distributions of box (or window) overlaps [130, 241]. This overlap is defined as usual, but restricted to a finite "window" of volume $l \times l \times l$, with $l < L$ fixed independently of the system size L. Note that for the aforementioned ferromagnet, the distribution of box overlaps converges to a pair of delta functions at $q = \pm 1$ when $L \to \infty$. For the $\pm J$ spin glass also the distribution of box overlaps turns out to remain non-trivial, in the same manner like the ordinary overlap.

Finally, we have also analyzed the distribution of link overlaps, see Eq. (11). In this case, the finite-size analysis [I] indicates a trivial distribution in the thermodynamic limit, which is not compatible with the MF picture of RSB [103], but on the other hand a non-trivial two-peak structure is also compatible with the data. Hence in this case the situation is not clear.

To summarize, the three-dimensional $\pm J$ model exhibits either a trivial ground-state landscape, or the non-trivial subspace has a very small weight. For finite temperatures, the behavior appears to be non-trivial, but not fully compatible with the MF scenario. The results obtained so far are compatible with the TNT picture [116, 117, 243] discussed above.

4 Vertex covers

In the previous chapters, we have studied physical models using sophisticated algorithms from computer science. In this section, we are considering the "opposite case", where methods and concepts from statistical physics contribute to a better understanding of problems from (theoretical) computer science.

For purely deterministic computers, all algorithms for solving problems from NP-c known currently need in the worst case an exponentially growing running time. Hence, it appears that the problems from NP-c are hard as well. So far there is no *proof* that the problems from NP are indeed hard. This is the P-NP problem, one of the great open questions in computer science. Translating the P-NP problem in natural language, means to answer the question "what is it that makes a problem hard?"

A notable advance [244, 245, 246] towards the answer of this question has recently occurred by realizing that the worst case and the typical case are different. This means that for some problems there are ensembles of random problem instances which can be solved typically in polynomial time, while the worst case is still exponential. There are suitably parametrized ensembles, for example random graphs or random boolean formulas, where in one region of parameter space the instances are easy while in another region the instances are hard [247, 248]. The instances, which are hardest to solve, are often found *at* the boundaries separating these regions. Hence, when studying the problems near the boundaries, one can hope to learn a lot about the reason for the hardness of the NP-c problems. Furthermore, the effects found at the boundaries have much in common with phase transitions in physical systems [3, 249]. As a consequence, methods from statistical physics [250], like the Replica trick or the cavity approach, have been applied to classical problems from computer science recently. The most prominent one is the satisfiability problem (SAT) [9]. SAT is one of the most fundamental problems in theoretical computer science. It was the first problem which was shown to be NP-complete, the proof was given by Cook in 1971 [251, 252]. Using the statistical mechanics approach it is possible to obtain results which have not been found before using classical mathematical methods [253, 254, 255, 256]. Furthermore this approach allows to invent new algorithms which are sometimes much faster than previously known algorithms [257].

Here, we concentrate on one model, the *vertex-cover* problem (VC), which belongs to the six basic NP-c problems in theoretical computer science. It has the advantage of being better accessible to a statistical mechanics analysis than SAT, furthermore it exhibits a physical interpretation as a hard-core lattice gas. After introducing the model, we present two algorithms which can be used to solve VC. In the succeeding section, we present results for the phase transition, which occurs when studying VC on an ensemble of random graphs. The results are summarized in a phase diagram obtained by using statistical mechanics methods. Finally, we show how the typical running time of an exact algorithm can be analyzed analytically by recurring on the results on the phase diagram.

4.1 Definition and basic results

Imagine you are director of a museum. In a first approximation, the museum consists of straight corridors, which meet at crossroads. Since the museum has a lot of precious artwork, you want to guard the museum by putting guards at the crossroads. We assume that a guard can observe all corridors adjacent to the crossroad. One can consider a museum as a graph, crossroads corresponding to vertices, corridors corresponding to edges. If we call the guarded crossroads and the adjacent corridors *covered*, then we arrive at the *vertex cover problem*.

Let us now give the mathematical definition of vertex covers. We take a graph $G = (V, E)$ with N vertices $i \in \{1, 2, ..., N\}$ and undirected edges $\{i, j\} \in E \subset V \times V$ connecting pairs of vertices. Note that $\{i, j\}$ and $\{j, i\}$ both denote the same edge.

We consider subsets $V' \subset V$ of vertices. These *vertices* are called *covered*, one can imagine a *covering mark* placed on it, see e.g. Fig. 13 (left). The *edges* adjacent to covered vertices are called covered as well. In case *all* edges are covered, i.e. if for all edges at least one of the endpoints is in V', one says the *graph* is covered and calls V' a *vertex cover*. The most simple vertex cover is obtained by choosing $V' = V$, but always smaller vertex covers exist, see Fig. 13 (right).

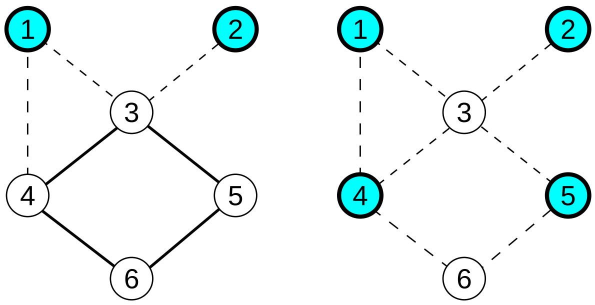

Figure 13: A sample graph. *Covered* vertices are shown in bold and dark, *covered* edges are indicated by dashed lines, uncovered edges by full lines. Left: Vertices 1 and 2 are *covered*. Thus, edges $(1, 3)$, $(1, 4)$, and $(2, 3)$ are *covered*. Right: by also covering vertices 4 and 5, the graph is covered, i.e. $V' = \{1, 2, 4, 5\}$ is a vertex cover.

In this context, one can study different kinds of problems. Either one fixes the number $X \equiv |V'|$ of available covering marks, corresponding to a given amount of money available to pay the guards. Now one can ask whether one can cover all edges, i.e. if it is possible to guard the museum completely. Or, if the number of covering marks is not sufficient, i.e. if the museum has not enough money, one can try at least to minimize the number of uncovered edges, i.e. to minimize the unguarded part of the museum[11] by placing the guards in an optimal way. On the other hand, one can allow arbitrary sizes of V' and look for the minimum-size vertex cover. This corresponds to the case where one wants to guard everything, but one wants to spent as less money as possible. In detail, the three main different variants of VC considered here are:

P1 The *minimal vertex-cover* problem consists in finding a vertex cover V' of minimal cardinality, and calculating the minimal fraction $x'(G) = |V'|/N$ of vertices needed to cover the whole graph.

P2 The *decision variant* of this problem is: "Given a number $X = xN$, is there a vertex cover V' of size X?".

P3 If there is no vertex cover of size X, one can study the related *optimization problem*: Find a set V' with $|V'| = X$ which minimizes the number of uncovered edges. In this case, we can assign an energy to each configuration

$$E(G, x) = \min\{\text{number of } \textit{uncovered} \text{ edges for } |V'| = xN\} \tag{19}$$

This means, the graph is coverable using $X = xN$ vertices iff the ground state energy is zero.

The proof of the NP-completeness of VC can be found in [9]. It works by mapping the above mentioned SAT problem onto VC.

In order to speak of median or average cases, and of phase transitions, we have to introduce a probability distribution over graphs. This can be done best by using the concept of *random graphs* as already introduced about 40 years ago by Erdös and Rényi [258]. A random graph $G_{N,p}$ is a graph with N vertices $V = \{1, ..., N\}$, any pair of vertices is connected randomly and independently by an edge with probability p. So the expected number of edges becomes $p\binom{N}{2} = pN^2/2 + O(N)$, and the average connectivity of a vertex equals $p(N-1)$.

The regime we are interested in consists, however, of *finite-connectivity graphs* in the large-N limit, i.e. those having $p = c/N$ with constant c. Then the average connectivity $c + O(N^{-1})$ stays finite. In this case, we also expect the size of minimal vertex covers to depend only on c, $x_{\mathrm{c}}(G) = x_{\mathrm{c}}(c)$ for almost all random graphs $G_{N,c/N}$.

In Computer Science/ Mathematics, previously some rigorous upper and lower bounds on $x_{\mathrm{c}}(c)$ where obtained [259, 260, 261], while the correct asymptotics for large c was given by Frieze [262]. To our knowöedge, the first calculation of the exact value of $x_{\mathrm{c}}(c)$ for small connectivities, was performed within this work and is presented below.

[11] To first approximation, all corridors have the same length and contain artwork of the same value.

4.2 Algorithms

There are two types of algorithms: incomplete and complete ones. Complete algorithms guarantee to find the optimum or true solution, hence the solution space is searched in principle completely. For incomplete algorithms, also called heuristics, it is not ensured that the true solution or the global optimum is found. Anyway, they are very often sufficient for practical applications.

First, a greedy heuristic for finding small vertex covers is discussed, i.e. it gives an approximation for the solutions of problem P1. The basic idea of the heuristic is to cover as many edges as possible by using as few vertices as necessary. Thus, it is favorable to cover vertices having a high degree. This step can be iterated, while the degree of the vertices is adjusted dynamically by removing edges and vertices which are covered. The algorithm returns an approximation $V_{\rm vc}^{\star}$ of the minimum vertex cover, the size $|V_{\rm vc}^{\star}|$ is an upper bound of the true minimum vertex-cover size. It is easy to invent examples where the heuristic fails to find the true minimum VC, e.g. a star graph having one center vertex to which $k > 2$ arms of length 2 are attached, see Fig. 14.

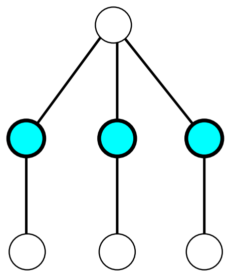

Figure 14: A small sample graph with minimum vertex cover of size 3. The vertices belonging to the minimum $V_{\rm vc}$ are indicated by dark/bold circles. For this graph the heuristic fails to find the true minimum cover, because is starts by covering the root vertex, which has the highest degree 3.

Next, we present two complete algorithms, hence they guarantee to find the exact answer.

First we turn to the problem, where we are interested only in minimum-size vertex covers (problem P1). Since each vertex can be either covered or uncovered, the most direct approach is to enumerate all possible 2^N configuration and choose among all covers that have the minimum size. Obviously, the time-complexity of this approach is $O(2^N)$. Early attempts [263, 264] have the same worst-case running time. The approach of Tarjan and Trojanowski [265] presented here has an $O(2^{n/2})$ time complexity. It uses an *divide-and-conquer approach*: First, all connected components of the graph are obtained. Then the method determines the minimum-size vertex covers for all components separately by recursive calls. The treatment of each connected component is based on the following idea. For each vertex, to obtain a vertex cover of the graph, one has either to cover the vertex or to cover all its neighbours. In both cases, one can remove the covered edges, search for a vertex cover in the remaining graph recursively, and take the smallest cover found as the output of the algorithm.

Furthermore, the algorithm uses the concept of *domination*. This means basically that one considers small subgraphs S. Among all possible covers of the subgraph one disregards those possibilities, which lead for sure not to better full covers but which cover only few or none of the edges connecting vertices from S and from $V \setminus S$. Due to the application of domination, the algorithms run faster than an exhaustive method, but it is just able to find *one* minimum cover, hence it cannot enumerate all solutions. One obtains the most simple example for domination when considering leaves, i.e. vertices i having only one neighbor j_1. Here, for a minimum-size vertex cover one must either cover i or j_1. Since i has only one neighbor, but j_1 possibly more, one can immediately cover j_1 and remove the vertices i, j_1 and all edges adjacent to them. This is the basic idea of the leaf-removal algorithm of Bauer and Golinelli [266].

The full algorithm of Tarjan is still deterministic but more general than leaf removal. It works as follows: For each connected component, the vertex i_0 having the smallest degree is determined. Degree $d_{i_0} = 0$ corresponds to an isolated vertex, which is not covered. Degree $d_{i_0} = 1$ corresponds to a leave which is treated as discussed above. Furthermore, the algorithm treats explicitly the cases of degrees d_{i_0} =2, 3 and 4. For higher lowest degrees $d_{i_0} > 4$, basically the subproblems for i_0 covered and i_0 uncovered must be treated completely. During the recursive calls generated in this way, the cases with smaller minimum degree might appear again. The full detailed five page presentation of the algorithm with all cases and subcases can be found in Ref. [265].

A more recent algorithm, which is simpler to implement [267], exhibits an even better time complexity $O(2^{n/2.863})$, and the authors claim that within their computer experiments it was actually faster than the method of Tarjan and Trojanowski.

If one is not only interested in one minimum vertex cover but in enumerating all solutions, then the divide-and-conquer method does not work and *Branch-and-Bound* approach [268, 269] must be applied. Also for the case where the number of covering marks X is given and one looks for all configuration of minimum energy (problem P3), a Branch-and-Bound method is feasible. We will present now an algorithm for this case. The Branch-and-Bound algorithm for enumerating all minimum-size covers (problem P1) works in the same way.

The Branch-and-Bound approach differs from the previous method by the fact that the concept of domination is not used. The basic idea is to build the full configuration (or *backtracking*) tree. While doing this, the algorithm makes certain choices where to put covering marks. If no cover is found, some covering marks have to be removed and to be placed elsewhere, i.e. the algorithm has to backtrack. This is done in a systematic way allowing to investigate the full configuration space. This $O(2^N)$ running time is reduced by omitting subtrees of the full tree by using a *bound*: Trees where for sure no minimum-energy configuration is located can be omitted. The bound applied in the following algorithm uses the *current* vertex degree d_i, which is the number of uncovered neighbors at a specific stage of the calculation. By covering a vertex i the total number of uncovered edges is reduced by exactly d_i. If several vertices $j_1, j_2, \ldots, j_k$ are covered, the number of uncovered edges is *at most* reduced by $d_{j_1} + d_{j_2} + \ldots + d_{j_k}$, the maximum reduction is only attained, when there is no edge running between any of the vertices $j_1, j_2, \ldots, j_k$. Assume that at a certain stage within the backtracking tree, there are *uncov* edges uncovered and still k vertices to cover. Then a lower bound M for the minimum number of uncovered edges in the subtree is given by

$$M = \max\left[0, uncov - \max_{j_1,\ldots,j_k} d_{j_1} + \ldots + d_{j_k}\right] . \tag{20}$$

The algorithm can avoid branching into a subtree if M is strictly larger than the number *opt* of uncovered edges in the best solution found so far.

For the order the vertices are selected to be (un-)covered within the algorithm, the following heuristic is applied: the order of the vertices is given by their current degree. Thus, the first descent into the tree is equivalent to the greedy heuristic presented before. Later, it will be become clear from the results that this heuristic is indeed a useful strategy.

In the actual implementation, the algorithm does not descend further into the tree as well, when no uncovered edges are left. In this case the vertex covers of the corresponding subtree consist of the vertices covered so far and all possible selections of k vertices among all uncovered vertices.

4.3 Phase diagram

4.3.1 The cover-uncover transition

First, the VC variant is considered where the energy is to be minimized for fixed values $x = X/N$ (problem P3). We know that for small values of x, the energy (19) is not zero [$e(0) = c/2$], i.e. no vertex covers exist, where xN vertices are covered. On the other hand, for large values of x, the random graphs are almost surely coverable, i.e. $e(x) = 0$. In Fig. 15 the average ground-state energy and the probability $P_{\text{cov}}(x)$ that a graph is coverable with xN vertices is shown for different system sizes (average connectivity $c = 2.0$). The results [J, 270] were obtained using the Branch-and-Bound algorithm, which was presented in the last section. As expected, the value of $P_{\text{cov}}(x)$ increases with the fraction of covered vertices. With growing graph sizes, the curves become steeper. This indicates that in the limit $N \to \infty$, which we are interested in, a sharp threshold $x_c \approx 0.39$ appears. Above x_c a graph is coverable with probability one, below it is almost surely not coverable. Thus, a phase transition from an uncoverable phase to a coverable phase occurs. The value x_c of the critical threshold depends on the average connectivity. The result for the phase boundary x_c as a function of c obtained by simulations is shown in reprint [J].

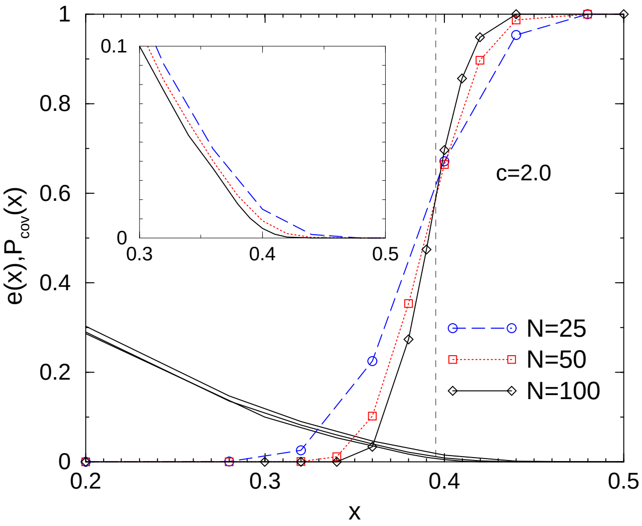

Figure 15: Probability $P_{\rm cov}(x)$ that a cover exists for a random graph ($c = 2$) as a function of the fraction x of covered vertices. The result is shown for three different system sizes $N = 25, 50, 100$ (averaged for $10^3 - 10^4$ samples). Lines are guides to the eyes only. In the left part, where the $P_{\rm cov}$ is zero, the energy average e (see text) is displayed. The inset enlarges the result for the energy in the region $0.3 \le x \le 0.5$.

In Fig. 16 the median running time of the Branch-and-Bound algorithm is shown as a function of the fraction x of covered vertices. The running time is measured in terms of the number of nodes which are visited in the backtracking tree. Again graphs with $c = 2.0$ were considered and an average over the same realizations as before was performed. A sharp peak can be observed near the transition x_c. This means, the instances which are the hardest to solve can be found near the phase transition. For values $x < x_c$, the running time still increases exponentially, as can been seen from the inset of Fig. 16. For values x considerably larger than the critical value x_c, the running time is linear. The reason is that the heuristic is already able to find a VC, i.e. the algorithm terminates after the first descent into the backtracking tree[12].

In physics, phase transitions are usually indicated by a divergence of measurable quantities such as specific heat or magnetic susceptibilities. The peak appearing in the running time serves as a similar indicator.

For small values of x in the uncoverable region, the running time is also faster

[12]The algorithm used here terminates after a full cover of the graph has been found since it is not necessary to enumerate all solutions

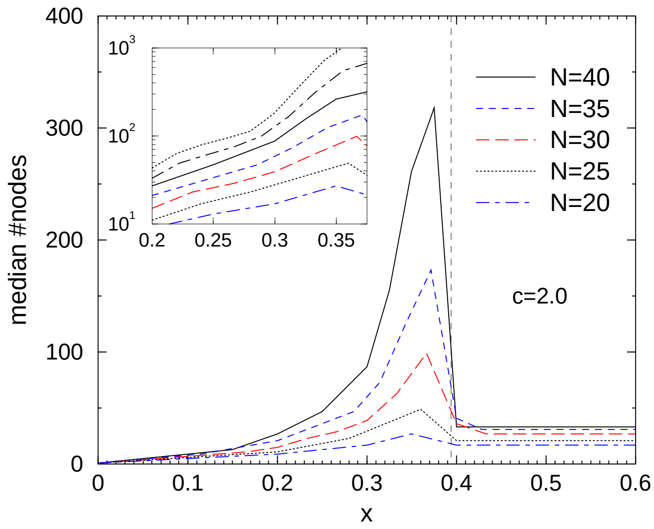

Figure 16: Running time of the Branch-and-Bound algorithm. Median number of nodes visited in the backtracking tree as a function of the fraction x of covered vertices for graph sizes $N = 20, 25, 30, 35, 40$ ($c = 2.0$). The inset shows the region below the threshold with logarithmic scale, including also data for $N = 45, 50$. The fact that in this representation the lines are equidistant shows that the running time grows exponentially with N.

than near the phase transition, but still grows exponentially. This is due to the fact that a configuration with a minimum number of *uncovered* edges has to be obtained, i.e. problem P3 has to be solved. If only the question whether a VC exists or not is to be answered (problem P2), the algorithm can be easily improved[13], such that for small values of x again a polynomial running time will be obtained.

4.3.2 Mapping to hard-core lattice gas

The phase diagram denotes the regions in the $c - x$ plane, where VC is coverable respectively were it is uncoverable. Hence, the separating line gives the value of the critical threshold x_c as a function of the connectivity c. Next, the analytic approaches applied in this work to obtain $x_c(c)$ are summarized.

For low connectivities $c < 1$ almost all vertices are contained in finite trees T_k of size k [258, 271]. Then one can calculate $x_c(c)$ using a cluster expansion, i.e. by explicitly calculating $x_c(T_k)$ for small k and weighting the results with the contribution of each tree T_k to the ensemble of random graphs. In Ref. [270] this expansion has been performed up to tree size $k = 7$, resulting in very good agreement with the numerical data for small connectivities $c < 0.3$.

[13] Set *best* := 0 initially.

By using a statistical mechanics approach it is even possible to derive an *exact* solution, which is furthermore valid even beyond the percolation threshold $c = 1$. It turns out that the solution is valid till $c = e$, where e is the Eulerian constant. The statistical mechanics treatment is outlined now. In the following subsection, the results will be presented, compared with the numerical findings and the structure of the phase diagram will be explained using four different percolation transitions occurring in VC on random graphs.

To study VC using concepts and methods of statistical mechanics, one has to map the problem onto a physical system. One possibility is to identify each vertex with an Ising spin and the two states *covered/uncovered* with the two spin orientations ± 1 [J]. Then the system can be studied in the canonical ensemble and the natural choice for the Hamiltonian is to identify the energy with the number of uncovered edges (19). Hence, vertex covers are ground states of the Hamiltonian.

Here a different mapping will be presented, where VC is mapped onto a hard-core lattice gas [K], since it allows for a simpler treatment. Any subset $U \subset V$ of the vertex set can be encoded by a configuration of N binary variables:

$$x_i := \begin{cases} 0 & \text{if} \quad i \in U \\ 1 & \text{if} \quad i \notin U \end{cases} \tag{21}$$

The choice of setting x_i to zero for vertices contained in U becomes clear if we look at the vertex cover constraint: An edge is covered by the elements in U iff at most one of the two end-points has $x = 1$. So the variables x_i can be interpreted as occupation numbers of vertices by the center of a particle. The covering constraint translates into a hard-sphere constraint: If a vertex is occupied, *i.e.* $x_i = 1$, then all neighboring vertices have to be empty. This can be described by an indicator function

$$\chi(x_1, ..., x_N) = \prod_{\{i,j\} \in E} (1 - x_i x_j) \tag{22}$$

which is one whenever $\vec{x} = (x_1, ..., x_N)$ corresponds to a vertex cover, and zero else. Having in mind this interpretation, we may write down the grand partition function

$$\Xi = \sum_{\{x_i = 0,1\}} \exp\left(\mu \sum_i x_i\right) \chi(\vec{x}) \tag{23}$$

with μ being a chemical potential which can be used to control the particle number, or the cardinality of U.

For regular lattices, this model is well studied as a lattice model for the fluid-solid transition, for an overview and the famous corner-transfer matrix solution of the two-dimensional hard-hexagon model by Baxter, see Ref. [272]. Recently, lattice-gas models with various kinds of disorder have been considered in connection with glasses [273, 274, 275] and granular matter [276, 277, 278, 279, 280, 281].

Minimal vertex covers correspond to particle packings of maximum density. Considering the weights in (23), it becomes obvious that the density $\nu(\mu)$ is an increasing function of the chemical potential. Highest density packings, or minimal vertex covers, are thus obtained in the limit $\mu \to \infty$:

$$x_c(c) = 1 - \lim_{\mu \to \infty} \nu(\mu) \ . \tag{24}$$

The fundamental step within the statistical mechanics approach is to calculate the grand partition function (23), from which the average density can be obtained by taking the derivative with respect to μ. The main steps of the calculation are applying the Replica trick [250], i.e. taking the disorder average over the n-th power of the partition function. Using a special 2^n-dimensional order parameter, one can rewrite the partition function as a functional integral over all possible normalized distributions of the order parameters. This integral can be evaluated using the saddle-point approximation, hence one has to make an ansatz for the order parameter distribution.

The simplest possibility is the replica-symmetric (RS) ansatz, which in our case assumes that the order parameter distribution depends only in a simple way on the order parameter. The resulting saddle-point equation can now be solved analytically in the limit of the chemical potential $\mu \to \infty$. The results are presented and discussed in the next subsection.

Before this, we discuss the assumption of replica symmetry. As it turns out [K] this assumption breaks down at average connectivity $c = e$, i.e. replica symmetry breaking occurs. Despite many efforts, the technical problem of handling RSB in finite-connectivity systems is still open. Most attempts [283, 284, 285, 286] try to apply the first step of Parisi's RSB scheme (1-RSB) [250] which, however, is technically well-understood only in the case of infinite-connectivity spin glasses. Due to a more complex structure of the order parameter in finite connectivity systems, a complete analytical solution is still missing. Recently, based on the connection to combinatorial optimization, the interest in this question was renewed [282], and some promising approximation schemes [255, 282] have been developed. Even more recently, a break-through was obtained in context of the cavity method [287]: Being more involved than the replica method in infinite-connectivity systems, the cavity approach becomes very elegant for finite connectivities. It allows for a straight-forward derivation of self-consistent order-parameter equations at a level, which is equivalent to 1-RSB, and these equations can be efficiently solved numerically using a population-dynamics algorithm. The cavity method has been recently [288] applied to VC by Zhou. He found that, although 1-RSB reproduces the numerical results above $c = e$ much better than the replica symmetric solution and satisfies numerically the bounds presented in Sec. 4.1, the 1-RSB solution is still not correct above $c = e$. Full RSB has to be included, which is a completely open technical issue. For this reason, we refer to Refs. [K, 288] for the technical details of our calculations and proceed with the presentation of the results, mainly for RS.

4.3.3 Phase boundary and percolation transitions

In this section, we give the analytical results of the statistical mechanics treatment, compare it with numerical simulations and discuss the morphology of the phase diagram, which can be characterized using four different percolation transitions occurring in the problem.

For the minimal vertex-cover size one obtains for the RS case

$$x_c(c) = 1 - \frac{2W(c) + W(c)^2}{2c} \; . \tag{25}$$

where $W(c)$ is the Lambert-W-function defined by $W(c)\exp(W(c)) = c$.

To calculate the phase boundary numerically, it is sufficient to calculate for each graph the size $X_{\mathrm{c}} = Nx_{\mathrm{c}}$ *one* minimum vertex cover. Hence one can apply the divide-and-conquer algorithm or the version of the Branch-and-Bound algorithm where X is not fixed. To compare with the analytical results one has to perform the thermodynamic limit $N \to \infty$ numerically. This can be achieved by calculating an average value $x_{\mathrm{c}}(N)$ for different graph sizes N. Then one fits a function

$$x_{\mathrm{c}}(N) = x_{\mathrm{c}} + aN^{-b} \tag{26}$$

to the data, where $x_c(\infty) = x_c$ ($b > 0$). The form of the function is purely heuristic, but works well.

Extremely good coincidence between analytical and numerical data is found for small connectivities $c < e$, see also Fig. 3 of reprint [J]. Up to this value however, we expect the replica-symmetric result to be exact. This is astonishing, as the solution does not show any particular signature of the percolation transition of the underlying random graph at $c = 1$. Note that due to the application of statistical mechanics methods like the Replica trick and the replica-symmetric ansatz, the treatment presented above is mathematically not rigorous. Anyway, for $c < e$, the result (25) was recently proven to be exact [289] in a constructive way by analysing the leaf-reomval algorithm. For $c > e$ systematic deviations are visible. For large c, (25) even violates the bounds and the exactly known asymptotics mentioned in section 4.1, this is due to the appearance of RSB.

The results [K, 288] of the cavity-method (corresponding to 1-RSB) (not shown) are better than the RS solution since they are numerically compatible with the asymptotics and within the bounds. But still the 1-RSB solution is significantly different from the numerical extrapolations in the region $c > e$.

An important quantity for the understanding of the phase diagram is the so called *backbone*: Usually the minimum-size VC is degenerate, hence some vertices are in some solutions covered but uncovered in other solutions. Also, there are vertices which are in all solutions covered or which are in all solutions uncovered, i.e. frozen in a physical sense. These vertices are called backbone vertices. From the replica-symmetric solution, one can read off immediately [K] the fractions of vertices belonging to these two backbone types:

$$\begin{aligned} b_{uncov}(c) &= \frac{W(c)}{c} \\ b_{cov}(c) &= 1 - \frac{W(c) + W(c)^2}{c} \,. \end{aligned} \tag{27}$$

Numerically, the backbone can be calculated by enumerating all minimum-size vertex covers of each realization for different sizes N and extrapolating for $N \to \infty$ in a similar way like Eq. (26). For $c < e$ again a very good agreement between analytical and numerical results is found [K]. For for $c > e$, the failure of the RS approach is here even more obvious than when studying $x_c(c)$.

A detailed analysis [K] shows that vertices having a small degree are usually uncovered backbone vertices, while the high-degree vertices usually form the covered backbone. This justifies a posteriori the use of heuristic algorithm presented in Sec. 4.2.

Further results can be obtained when studying the subgraphs induced by the backbone and the non-backbone vertices [K]. It turns out that the structure of the non-backbone graphs in the low connectivity regime $c < e$ is as follows. They consists of a collection of pairs, which are the simplest graphs having no backbone. These pairs are connected by additional edges. These subgraphs show a percolation transition at $c_{\mathrm{bb}} = \exp(1/\sqrt{2})/\sqrt{2}$ with $1 < c_{bb} < e$. Hence the onset of RSB at $c = e$ *cannot* be explained by this percolation transition. A similar study for the backbone subgraphs shows that it percolates already at the original percolation threshold $c = 1$.

Nevertheless, Bauer and Golinelli have indeed related the onset of RSB to a fourth percolation transition [266]. They have applied the leaf-removal algorithm to find minimum-size VCs. The remaining graph, which is obtained once no more leaves are left, they call the *core*. They find that below $c = e$ the core splits into small disconnected components of logarithmic size, while above $c = e$ the core percolates. Hence, the percolation transition of the core seems responsible for the onset of RSB!

Finally, we note that within the replica-symmetric framework, it is not possible to calculate the entropy exactly, even not in the limit $\mu \to \infty$, one has to make a variational ansatz. Nevertheless, the resulting entropy agrees for $c < e$ well with the $N \to \infty$ extrapolations of the numerical results stemming from enumerations of all minimum-size vertex covers, see Ref. [K].

4.4 Analyzing algorithms

In theoretical computer science the time complexity of an algorithm is the asymptotic ($N \to \infty$) worst-case running time measured in some suitable unit on a model computer, i.e. an upper bound for the running time. In real-world applications one investigates usually not the worst-case problems but *typical* problems.

As we have seen in Sec. 4.3.1 there might be regions in parameter space, where VC is typically solved in polynomial time while it is typically hard elsewhere. Hence, one would like to observe this easy-hard transition within an analytical analysis as well. This would allow for a better understanding of the underlying mechanisms, hence a step towards answering the question "what is it that makes a problem hard?" Again a statistical mechanics treatment, in particular the knowledge of the phase diagram as calculated before, helps a great deal in this task.

The algorithm whose analysis is summarized here is a simplified version of the algorithm presented in Sec. 4.2. The reason for this simplification is that it allows for an analysis using simple analytical methods. In the course of the developments of more sophisticated methods during the next years, it should be possible to analyze more elaborate algorithms.

The simplified Branch-and-Bound algorithm does *not* use the greedy heuristic, instead the vertices are selected randomly among the vertices, which have not been assigned a state so far. Furthermore a simpler bound is used: The algorithm continues to branch into subtrees as long as the number of covered vertices does not exceed the given limit and as long no vertex cover has been found.

The type of analysis presented here was first applied to the 3-SAT problem by Cocco and Monasson [290]. The application to VC is presented in Ref. [L]. The analysis of the algorithm consists of two parts: first, the analysis of the first descent into the tree and, second, the calculation of the full running time, which includes backtracking in case no cover was found in the first descent. The running time is measured in terms of the number of nodes visited in the backtracking tree.

The first descent into the tree: Previously, probabilistic analysis of descent algorithms have been applied to establish rigorous bounds on phase boundaries [244, 246, 291]. The analysis of the first descent into the left-most subtree is straight forward for the algorithm presented here, as it forms a Markov process of random graphs: In every time step, one vertex and all its incident edges are covered and can be regarded as removed from the graph. As the order of appearance of the vertices is not correlated to its geometrical structure, the graph remains a random graph. After T steps, we consequently find a graph $G_{N-T,c/N}$ having $N-T$ vertices. As the edge probability remains unchanged, the average connectivity decreases from c to $(1-T/N)c$.

For large N, it is reasonable to work with the *rescaled time* $t=T/N$, which becomes continuous in the thermodynamic limit. In this notation, our generated graph reads $G_{(1-t)N,c/N}$. An isolated vertex is now found with probability $(1-c/N)^{(1-t)N-1}\simeq\exp\{-(1-t)c\}$, so the expected number of vertices which can be still covered (starting from X) becomes $X(t)=X-N\int_0^t dt'(1-\exp\{-(1-t')c\})$. The first descent thus describes a trajectory in the $c-x$-plane,

$$c(t) \quad = \quad (1-t)c \qquad (28)$$

$$x(t) \;=\; \frac{x-t}{1-t} + \frac{e^{-(1-t)c} - e^{-c}}{(1-t)c}.$$

The results are presented in Fig. 17. One observes a perfect agreement of the analytical result and the trajectory generated for a large graph.

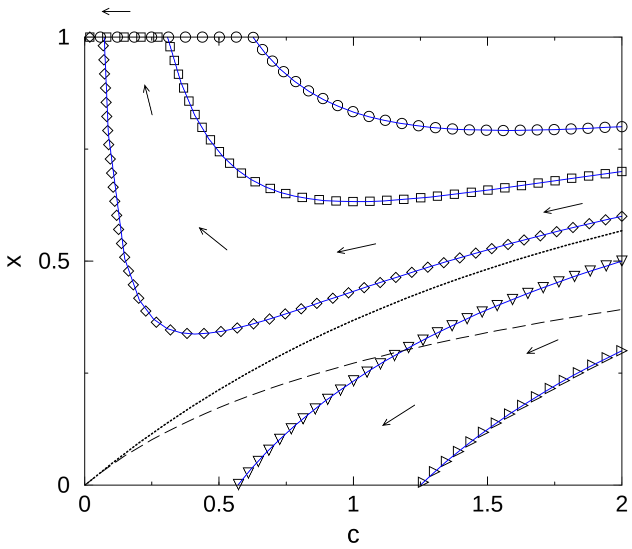

Figure 17: Trajectories of the first descent in the (c, x) plane. The full lines represent the analytical curves, the symbols numerical results of one random graph with 10^6 vertices, $c = 2.0$ and $x = 0.8$, 0.7, 0.6, 0.5 and 0.3, respectively. The trajectories follow the sense of the arrows. The dotted line $x_b(c)$ separates the regions where this simple algorithm finds a cover from the region where the method fails. No trajectory crosses this line. The long dashed line represents the true phase boundary $x_c(c)$, instances below that line are not coverable.

Analysis of the full algorithm: To understand how the backtracking algorithm works, we study the trajectories together with the phase diagram. We can observe three regions:

I The algorithm works in linear, i.e. polynomial time, if the first descent already finds a VC. This is the case for large starting value of x. Then $x(t)$ reaches the value one at a certain rescaled time $t < 1$, and the graph is proven to be coverable after having visited tN nodes of the backtracking tree. The critical value $x_{\rm b}(c)$ above which this happens can be obtained from (28) by setting $x(t) = 1$ and resolving with respect to x in the limit $t \to 1$:

$$x_{\rm b}(c) = 1 + \frac{e^{-c} - 1}{c} \tag{29}$$

II For $x_\mathrm{c}(c) < x < x_\mathrm{b}(c)$ the graph is typically coverable, but during the first descent $x(t)$ vanishes already before having covered all edges. The trajectory crosses the phase transition line at a certain rescaled time $\tilde{t}$ at $(\tilde{c}, \tilde{x})$. There the generated random subgraph of $\tilde{N} = (1-\tilde{t})N$ vertices and average connectivity $\tilde{c}$ becomes uncoverable by the remaining $\tilde{x}\tilde{N}$ covering marks. To determine that the generated subproblem is not coverable, the algorithm has basically to visit the full backtracking tree for the subproblem. Hence, exponential solution times have to be expected. This means $x_\mathrm{b}(c) > x_\mathrm{c}(c)$ denotes the easy-hard transition of the algorithm. After backtracking the region of the uncoverable subproblem, the algorithms proceeds until a solution is found.

III For $x < x_\mathrm{c}(c)$, the graph is typically not coverable. Thus, again the algorithm has to build a full backtracking tree until it is proven that no VC exists. Hence, again the running time is exponential.

To calculate the running time of the algorithm one has to calculate the size of the backtracking tree generated during the calculation. This size is determined by the numbers $\tilde{N}, \tilde{c}$ and $\tilde{x}$ characterizing the uncoverable subproblem which is typically generated. This calculation can be performed using an annealed approximation and by applying a saddle-point argument (i.e. the running time is exponentially dominated by the largest uncoverable subproblem generated). Details can be found in Ref. [L]. The result is displayed in Fig. 18, where it is compared with numerical simulations.

The algorithm exhibits a peak of the running time exactly at the phase boundary. This can be directly understood by looking again at Fig. 17: For $x > x_\mathrm{c}(c)$ the uncoverable subproblems, which have to be backtracked fully, are smaller than the full graph. For $x < x_\mathrm{c}(c)$, the number of vertices to cover is so small that the generated backtracking trees are smaller due to the trivial bound included in the algorithm. Hence, directly *at* the phase boundary the size of the backtracking tree is maximal.

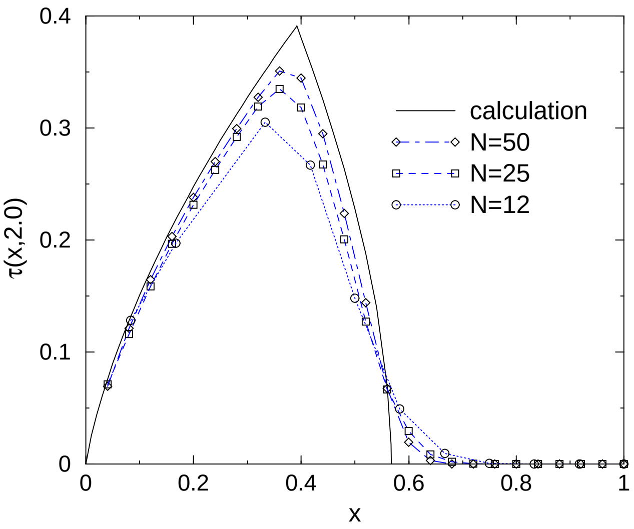

Figure 18: Normalized and averaged logarithm of the running time of the algorithm as a function of the fraction x of coverable vertices. The solid line is the result of the annealed calculation. The symbols represent the numerical data for $N = 12, 25, 50$, lines are guides to the eyes only.

5 Discussion and outlook

In this work, disordered systems from statistical physics and theoretical computer science were studied. On the one hand, it was the aim to obtain a better understanding of the physical behavior, i.e. of phase transitions and of the nature of the ordered phases. One the other hand, this work aims at better understanding the relation between physical complexity, represented here by glassy behavior, and computational complexity, captured in the notion of NP-completeness and culminating in the P-NP problem, i.e. in the question “What is it that makes a problem computationally hard”.

Although a full understanding of the low-temperature behavior of glassy systems and of the reason for computational hardness seems to be still far away, notable advance has been achieved in this work. First, by mapping random-field systems on networks and applying fast maximum-flow algorithms, ground states of large random-field system could be calculated exactly. This is due to the fact that obtaining ground states is a polynomial problem here. In three and higher dimensions, this model exhibits an ordered phase at low temperatures and small disorder. Since the critical behavior of this systems for finite temperatures can be inferred from the ground-state properties, by measuring several specific quantities, all critical exponents characterizing the phase transition could be calculated independently. All (hyper-) scaling relations are fulfilled, indicating that finite-size scaling techniques, originating from renormalization-group analysis, are also appropriate for disordered systems at least for the random-field case. But the behavior of the specific heat is different from the result found in experiments on diluted antiferromagnets in a field. So far it was believed that diluted antiferromagnets and random-field systems belong to the same universality class. Hence, the next step will be to study diluted antiferromagnets in the same way, since for this model exact ground states can be obtained also using a maximum-flow algorithm. It is only the appearance of discontinuities in the bond energy which has prevented performing this analysis so far. Additional methods for the data analysis are necessary here. Also the nature of the disordered phase at low temperatures just above the transition line is still unclear. Former Monte Carlo simulations indicated a behavior similar to spin glasses, while in other ground-state studies no indications for a complex phase were found. Here a combination of ground-state algorithms and dynamical simulations should illuminate the problem.

Second, the low-temperature behavior of spin glasses was studied. The ground-state problem is polynomial in two dimensions and NP-complete in three dimensions. This change of complexity is also reflected in the physical behavior. For two-dimensions, although each finite-size realization may exhibit a rich behavior, there is no stable spin-glass phase at finite temperatures and the low-temperature behavior is well described by the Droplet scaling picture, i.e. it is basically like in a (disordered) ferromagnet, but being described by different critical exponents.

In this work several fundamental predictions of the Droplet picture could be verified, by calculating ground states, domain-wall and droplet excitations and using the aspect-ratio scaling approach. The main result is that the full behavior of large systems is characterized by one single (domain-wall) exponent $\theta = -0.287$.

Although the behavior of two-dimensional systems seems clear in principle, several questions remain. First of all, the scaling corrections depend crucially on the way the excitations are generated, they are in some cases even fully absent. To understand this effect better, one could e.g. study the interactions of domain walls directly, analyse the first excitations of each system and generate "typical" excitations by simulations at small but finite temperatures using a cluster algorithm. Furthermore, the behavior of systems with other kind of interactions (parametrized mixture of ferromagnet, antiferromagnet and decoupled) or of non-planar two-dimensional systems, where the ground-state problem seems non-polynomial, is still not known well.

In three dimensions, it is now clear that an ordered low-temperature phase exists. The simple Droplet ansatz is not sufficient. The spin-glass phase is characterized by many features of the mean-field result, but not by all. Due to the NP-completeness of the problem, only medium-size systems can be studied so far. To be more sure about the results, better algorithms are needed to study larger systems. Also the behavior in a field and many dynamical properties are still not well understood. Thus, much work has to be done in the field of spin-glass physics in the near future

Spin-glass behavior can be found in models belonging to other fields, for example in problems from theoretical computer science. This is true in particular for the vertex-cover problem studied on an ensemble of random graphs, as in the previous chapter of this work. Using exact Branch-and-Bound algorithms and analytical techniques, we could achieve an understanding, which goes much beyond what has been known of this problem before from classical mathematical analysis. We studied the coverable-uncoverable phase transition, which coincides with a peak in the typical running time of the algorithm, obtain the phase diagram and understand its behavior in terms of four percolation transitions occurring in the model. Furthermore, we were able to study analytically the *typical* running time of a simple but exact algorithm, opposed to the results obtained before in theoretical computer science, which are only describing the *worst-case* behavior.

Although the occurrence of the hardest to solve instances is correlated very often with phase transitions, like in the vertex-cover problem here, the understanding of the conditions for computational hardness is still weak. It seems to be correlated to glassy behavior of the related physical models, hence a unifying concept of physical and computational complexity seems natural. In particular, for the vertex-cover problem, a better analysis of the solution space, e.g. by using a cluster analysis, will allow to obtain more insight. On the other hand, the application of physical methods allows to invent much faster algorithms, as recently demonstrated for the satisfiability problem by using a cavity approach. Only few problems have been analyzed in this field so far, but there are more than 10000 NP-complete problems. There is still a lack of a fundamental understanding, which goes beyond the investigation of single models. Anyway, to obtain this fundamental understanding, probably few other models have to be analysed in the same way. In addition to their static behavior, also dynamical properties, which can be inferred from Monte Carlo simulations, will allow for a thorough analysis. In the next step, the research should be extended to other complexity classes, e.g. the class of PP (probabilistic polynomial) problems which involve the application of statistical algorithms. Also relations to other fields, e.g. to biological complexity as present in the genome of living cell, offer uncountable many open problems and should be followed much more intensively. To summarize, one can say that the field of (physical, computational, biological, ...) complexity, to understand how many simple but interacting entities are able to behave in a complex manner, will be one of the most fruitful areas of research during the next few decades.

Appendix

Complexity Theory

For the moment, we will only consider recognition problems. These are problems for which only the answers “yes” or “no” are possible. An algorithm which *decides* a decision problem A, i.e. which halts on all input instances a and answers either “yes” or “no”, is called a *decision algorithm* for A.

The fundamental recognition problem in theoretical computer science is the satisfiability problem (SAT) [9]. Each instance of SAT consists of a boolean formula F over n logical variables $x_i = 0, 1$ and the question “Is there an assignment of the variables such that the formula evaluates to true?” The simplest algorithm to answer this question uses the fact that each formula contains a finite number n of variables. Therefore, there are exactly 2^n different assignments for the values of all variables. To check whether a formula is satisfiable, one can scan through all possible assignments and check whether the formula evaluates to true or to false. If for one assignment the formula is true, then it is satisfiable, otherwise not. Since for each formula up to 2^n assignments have to be tested, this general algorithm has an exponential time complexity (in the number of variables).

There are variants of SAT, which can be decided faster. The most common form is k-SAT, where the formulas consist of m *clauses* C_j combined by the AND operator $F = C_1 \wedge C_2 \wedge \ldots \wedge C_m$ and each clause consists of k negated or unnegated variables connect by the OR operator $\vee$. Now, for $k \leq 2$, a polynomial-time algorithm which decides whether F is satisfiable, is known, for more details see [251, 252]. Hence, both 1-SAT and 2-SAT belong to the following class of problems:

Definition: P (polynomial) The class P contains all recognition-problems for which there exists a polynomial-time decision algorithm.

Note that the term “polynomial” refers to the asympotic growth of the worst-case running time as a function of input size. Furthermore, in practical context, usually not only recognitions problems are considered as being members of P, but all problems having a polynomial-time algorithm to solve it.

The class NP of recognition problems will be defined next. For this purpose we use *certificate-checking* (CC) algorithms. These are algorithms $\mathcal{A}$ which get as input instances a (e.g. formulas) like decision algorithms and additionally strings $s = s_1 s_2 \ldots s_n$, called *certificates* (made from a suitable alphabet). Like decision algorithms they halt on all inputs (a, s) and return only “yes” or “no”. The meaning of the certificate strings will become clear from the following. A new class, called NP, can be described as follows:

The difference between P and NP is (see Fig. 19): for a yes-instance of a

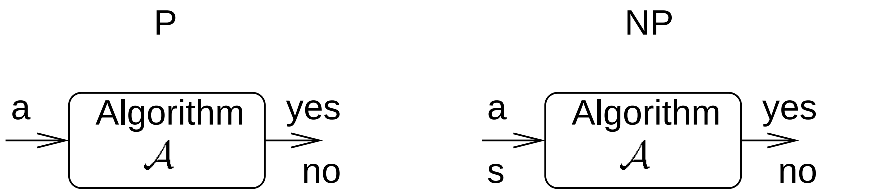

$a \in \mathrm{A} \Leftrightarrow \mathcal{A}(a) =$“yes“ $\qquad a \in \mathrm{A} \Leftrightarrow \exists s : \mathcal{A}(a, s) =$“yes“

Figure 19: Classes P and NP.

P problem the decision algorithm answers “yes”. For a yes-instance of an NP problem there *exists* at least one certificate-string s such that the CC algorithm answers “yes”, i.e. there may be many certificate strings s with $\mathcal{A}(a, s)$=“no” even if a is a yes-instance. For a no-instance of a P problem the decision algorithm answers “no”, while for a no-instance of an NP problem the CC algorithm answers “no” for *all* possible certificate strings s. As a consequence, P is a subset of NP, since every decision algorithm can be extended to a certificate-checking algorithm by ignoring the certificate. For the case of SAT, the certificate is an assignment of the variables and the CC algorithm evaluates a given formula with the given assignment.

The formal definition of NP is as follows:

Definition: NP (nondeterministic polynomial) A recognition-problem A is in the class NP, if there is a polynomial-time (in then length $|a|$ of the input) certificate-checking algorithm with the following property:

An instance a is a yes-instance if there is at least one certificate s with $\mathcal{A}(a, s)$=yes, for which the length $|s|$ is polynomial in $|a|$ ($\exists z : |s| \leq |a|^z$).

In fact, the requirement that the length of s is polynomial in $|a|$ is redundant, since the algorithm is allowed to run only a polynomial number of steps. During that time the algorithm can read only a certain number of symbols from s which cannot be larger than the number of steps itself. Nevertheless, the length-requirement on s is included for clarity in the definition.

The name “nondeterministic polynomial” comes from the fact that one can show that a *nondeterministic algorithm* can decide NP problems in polynomial time. A normal algorithm is deterministic, i.e. from a given *state* of the algorithm, which consists of the values of all variables and the program line where the execution is at one moment, the next state follows in a deterministic way. Nondeterministic algorithms are able to choose the next state randomly. Thus, a machine executing nondeterministic algorithms is just a theoretical construct, but in reality cannot be built yet[14]. The definition of NP relies on certificate-checking algorithms. For each CC algorithm an equivalent nondeterministic algorithm can be formulated in the following way. The steps where a CC algorithm reads the certificate can be replaced by the nondeterministic changes of state. An instance is a yes-instance if there is at least one run of the nondeterministic algorithm which answers "yes" with the instance as input. Thus, both models are equivalent.

As we have stated above, different recognition problems can be mapped onto each other. Since all algorithms which we encounter in this context are polynomial, only transformations are of interest which can be carried through in polynomial time as well (as a function of the length of an instance). The precise definition of the transformation is as follows:

Definition: Polynomial-time reducible Let A, B be two recognition problems. We say A is *polynomial-time* reducible to B ($A \leq_p B$), if there is a polynomial-time algorithm f such that

$$x \text{ is yes-instance of A} \quad \Leftrightarrow \quad f(x) \text{ is yes-instance of B}$$

Fig. 20 shows how a certificate-checking algorithm for B can be transformed into a certificate-checking algorithm for A using the polynomial-time transformation f.

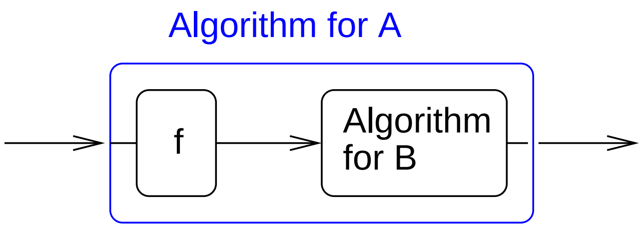

Figure 20: Polynomial-time reducibility: a certificate-checking algorithm for problem A consisting of the transformation f and the algorithm for B.

There is a special subset of NP problems which reflects in some sense the general attributes of all problems in NP: it is possible to reduce all problems of NP to them. This leads to the following definition:

Definition: NP-completeness The recognition problem $A \in$ NP is called *NP-complete* if all problems B∈NP are polynomial reducible to A:

$$\forall\, B \in \mathrm{NP}: B \leq_p A$$

[14]Quantum computers can be seen as a special realization of nondeterministic algorithms, but they have not the full power of a true nondeterministic algorithm.

It can be shown that SAT is NP-complete. The proof is quite technical. It requires an exact machine model for certificate-checking algorithms. The basic idea is: each problem in NP has a certificate-checking algorithm. For that algorithm, a given instance and a given certificate, an equivalent boolean formula is constructed which is only satisfiable if the algorithm answers "yes" given the instance and the certificate. For more details see [252, 292, 293].

Since SAT is NP-complete, A$\leq_p$SAT for every problem A$\in$NP. One can show. SAT$\leq_p$3-SAT. Since the $\leq_p$-relation is transitive, we obtain A$\leq_p$3-SAT. Consequently, 3-SAT is NP-complete as well. There are many other problems in NP which are NP-complete. For a proof it is sufficient to show A$\leq_p$B for any other NP-complete problem A, e.g. 3-SAT$\leq_p$B. A list of known NP-complete problems is growing permanently. Several of them can be found in [9].

As we said above, P is a subset of NP. If for one NP-complete problem a polynomial-time decision algorithm was be found, then, using the polynomial time reducibility, this algorithm could decide *every* problem in NP in polynomial time. Consequently, P=NP would hold. *Not for a single* problem from NP, a polynomial-time decision algorithm has been found so far. Hence, it is very likely that no polynomial-time algorithms exists. On the other hand, it has not been possible so far to prove that no such algorithm exists. Therefore the so called P-NP-problem, whether P$\neq$NP or P=NP, is still unsolved, but P=NP seems to be very unlikely. We can draw everything that we know about the different classes in a figure: NP is a subset of the set of decidable problems, i.e. one can answer "yes" or "no" for each instance. The NP-complete problems are a subset of NP. P is a subset of NP too. If we assume P$\neq$NP, then problems in P are not NP-complete. Finally we should mention that there are recognition problems which cannot be decided, only proven[15] (see Fig. 21).

In this section we have concentrated on recognition problems. Optimization problems are not recognition problems since one tries to find a configuration $\underline{\sigma}$ minimizing or maximizing a cost function $H(\underline{\sigma})$. This is not a question that can be answered by "yes" or "no". Howevery, every problem of finding $\min H(\underline{\sigma})$ can be transformed into a recognition problem of the form

"given a value K, is there an configuration $\underline{\sigma}$ with $H(\underline{\sigma}) \leq K$?"

In this way one can classify also optimization problems according the classes P and NP.

[15]A problen can be proven, if there is a algorithm, which halts and answers "yes" in case of a "yes"-instance, but for a "no" instance the algorithm may not halt, i.e. will run forever. An example is the "halting" problem: "Will a given algorithm halt on a given input?"

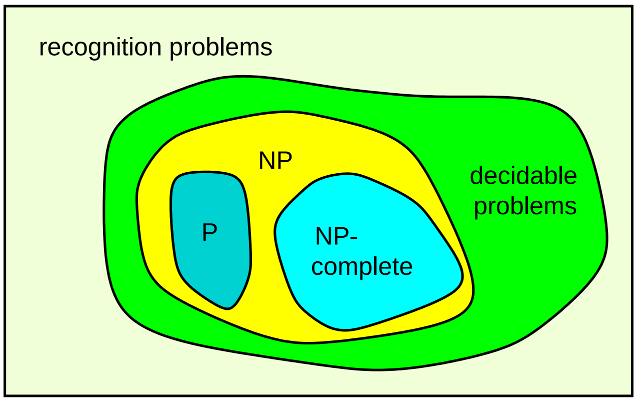

Figure 21: Relation between different classes of recognition problems.

References

Original contributions involving the author, reprinted at the end

Refs. [A] to [I] contain purely numerical work, which were completely performed by A.K. Hartmann, except that the results for full periodic boundary conditions in Ref. [E] were obtained by the coauthor and few results in Ref. [D] were taken from [161]. Refs. [J] to [L] contain both analytical and numerical work. Here A.K. Hartmann performed the numerical work. For all papers all authors contributed ideas to the work and participated in writing the paper.

[A] A.K. Hartmann and A.P. Young, Phys. Rev. B **64**, 214419 (2001)

[B] A.K. Hartmann, Phys. Rev. B **65**, 174427 (2002)

[C] A.K. Hartmann and A.P. Young, Phys. Rev. B **64**, 180404 (2001)

[D] A.K. Hartmann, A.J. Bray, A.C. Carter, M.A. Moore, und A.P. Young, Phys. Rev. B **66**, 224401 (2002)

[E] A.K. Hartmann and A.P. Young, Phys. Rev. B **66**, 094419 (2002)

[F] A.K. Hartmann and M.A. Moore, Phys. Rev. Lett. **90**, 127201 (2003)

[G] A.K. Hartmann, J. Phys. A **33**, 657 (2000)

[H] A.K. Hartmann, Eur. Phys. J. B **13**, 539 (2000)

[I] A.K. Hartmann and F. Ricci-Tersenghi, Phys. Rev. B **66**, 224419 (2002)

[J] M. Weigt and A.K. Hartmann, Phys. Rev. Lett. **84**, 6118 (2000)

[K] M. Weigt and A.K. Hartmann, Phys. Rev. E **63**, 056127 (2001)

[L] M. Weigt and A.K. Hartmann, Phys. Rev. Lett. **86**, 1658 (2001)

Other references

[1] D.J. Amit, *Field Theory, The Renormalization Group and Critical Phenomena*, (World Scientific, Singapore 1984)

[2] D. Chandler, *Introduction to Modern Statistical Mechanics*, (Oxford University Press, Oxford 1987)

[3] J.M. Yeomans, *Statistical mechanics of Phase transitions*, (Oxford University Press, 1992)

[4] J. Cardy, *Scaling and Renormalization in Statistical Physics*, (Cambridge University Press 1996)

[5] L.E. Reichl, *A Modern Course in Statistical Physics*, (John Wiley & sons, New York 1998)

[6] L. van Hemmen and I. Morgenstern (ed.), *Heidelberg Colloqium on Glassy Dynamics*, (Springer, Heidelberg 1986)

[7] A.K. Hartmann and H. Rieger, *Optimization Algorithms in Physics*, (Wiley-VCH, Berlin, 2001)

[8] S. Kirkpatrick, C.D. Gelatt and M.P. Vecchi M P, Science **220**, 671 (1983)

[9] M.R. Garey and D.S. Johnson, Computers and Intractability, (Freeman, San Francisco, 1979)

[10] Y. Imry and S.-K. Ma, Phys. Rev. Lett. **35**, 1399 (1975).

[11] D.P. Belanger and A.P. Young, J. Magn. and Magn. Mat. **100**, 272 (1991)

[12] H. Rieger, in: D. Stauffer (ed.), *Annual Reviews of Computational Physics II*, (World Scientific, Singapore 1995)

[13] A.P. Young (ed.), *Spin Glasses and Random Fields*, (World Scientific, Singapore 1998)

[14] K. Binder and A.P. Young, Rev. Mod. Phys. **58**, 801 (1986)

[15] M. Mezard, G. Parisi, and M.A. Virasoro, *Spin Glass Theory and Beyond*, (World Scientific, Singapore 1987)

[16] K.H. Fisher and J.A. Hertz, *Spin Glasses*, (Cambridge University Press, Cambridge 1991)

[17] J.A. Mydosh, *Spin Glasses: an Experimental Introduction*, (Taylor and Francis, London 1993)

[18] S. Fishman and A. Aharony, J. Phys. C **12**, L729 (1979)

[19] J.L. Cardy, Phys. Rev. B **29**, 505 (1984)

[20] D.P. Belanger, A.R. King, V. Jaccarino and J.L. Cardy, Phys. Rev. B **28**, 2522 (1983)

[21] D.P. Belanger and Z. Slanič, J. Magn. and Magn. Mat. **186**, 65 (1998)

[22] D.P. Belanger, in *Spin Glasses and Random Fields*, A.P. Young (Ed.), 251 (World Scientific, 1998)

[23] U. Nowak and K.D. Usadel, Phys. Rev. B **39**, 2516 (1989)

[24] U. Nowak and K.D. Usadel, Phys. Rev. B **44**, 7426 (1991)

[25] K.D. Usadel and U. Nowak, JMMM **104-107**, 179 (1992)

[26] T. Nattermann, in *Spin Glasses and Random Fields*, A.P. Young (Ed.), 277 (World Scientific, 1998)

[27] A. Aharony, Y. Imry, and S.K. Ma, Phys. Rev. Lett. **37**, 1364 (1976)

[28] A.P. Young, J. Phys. C **10**, L257 (1977)

[29] G. Parisi and N. Sourlas, Phys. Rev. Lett. **43**, 744 (1979)

[30] M. Aizenman and J. Wehr, Phys. Rev. Lett. **62**, 2503 (1989)

[31] J. Bricomont and A. Kupiainen, Phys. Rev. Lett. **59**, 1829 (1987)

[32] J.R.L. de Almeida and R. Bruinsma, Phys. Rev. B **35**, 7267 (1987)

[33] M. Mézard and A.P. Young, Europhys. Lett. **18**, 653 (1992)

[34] M. Guagnelli, E. Marinari and G. Parisi, J. Phys. A **26**, 5675 (1993)

[35] M. Mézard and R. Monasson, Phys. Rev. B **50**, 7199 (1994)

[36] D. Lancaster, E. Marinari, and G. Parisi, J. Phys. a **28**, 3959 (1995)

[37] E. Brézin and C. de Dominics, Europhys. Lett. **44**, 13 (1998)

[38] J. Esser and U. Nowak, Phys. Rev. B **55**, 5866 (1997)

[39] D.P. Landau and K. Binder, *A Guide to Monte Carlo Simulations in Statistical Physics*, (Cambridge University Press, Cambridge 2000).

[40] J. Sinova and G. Canright, Phys. Rev B **64**, 094402 (2001)

[41] A.A. Middleton and D.S. Fisher Phys. Rev. B **65**, 134411 (2002)

[42] T. Schneider and E. Pytte Phys. Rev. B **15**, 1519 (1977)

[43] A. Aharony, Phys. Rev B **18**, 3318 (1978)

[44] G. Grinstein, Phys. Rev. Lett. **34** 944 (1976)

[45] A.J. Bray and M.A. Moore, J. Phys. C **18** L927 (1985)

[46] J. Villain, J. Physique **46**, 1843 (1985)

[47] D.S. Fisher, Phys. Rev. Lett. **56**, 416 (1986)

[48] M. Schwartz and A. Soffer, Phys. Rev. Lett. **55**, 2499 (1985)

[49] M. Schwartz, J. Phys. C **18**, 135 (1985); M. Schwartz and A. Soffer, Phys. Rev. B **33**, 2059 (1986); M. Schwartz, M. Gofman, and T. Nattermann, Physica A **178**, 6 (1991); M. Schwartz, Europhys. Lett. **15**, 777 (1994)

[50] H. Rieger, Phys. Rev B **52**, 6659 (1995)

[51] M.E.J. Newman and G.T. Barkema, Phys. Rev. B **53**, 393 (1996)

[52] J.-C. Picard and H.D. Ratliff, *Networks* **5**, 357 (1975)

[53] A.T. Ogielski, *Phys. Rev. Lett.* **57**, 1251 (1986)

[54] J.C. Anglès d'Auriac, M. Preissmann and A. Seb, J. Math. and Comp. Model. **26**, 1 (1997)

[55] H. Rieger, in: *Advances in Computer Simulation*, Ed. J. Kertesz and I. Kondor, Lecture Notes in Physics **501**, (Springer, Heidelberg, 1998)

[56] M.J. Alava, P.M. Duxbury, C. Moukarzel and H. Rieger, in Ed. C. Domb and J.L. Lebowitz, *Phase transitions and Critical Phenomena*, **18**, (Academic press, New York 2001)

[57] J.-C. Picard and M. Queyranne, *Math. Prog. Study* **13**, 8 (1980)

[58] A.K. Hartmann and K.D. Usadel, *Physica A* **214**, 141 (1995)

[59] A.K. Hartmann, Physica A **248**, 1 (1998)

[60] S. Bastea and P.M. Duxbury, *Phys. Rev. E* **58**, 4261 (1998)

[61] E.T. Seppälä, M.J. Alava, and P. M. Duxbury, Phys. Rev. E **63**, 036126 (2001)

[62] E.T. Seppälä and M.J. Alava, *Phys. Rev. Lett.* **84**, 3982 (2000)

[63] E.T. Seppälä, V.I. Raisanen, and M.J. Alava, Phys. Rev. E **61**, 6312 (2000)

[64] R. Fisch, *J. Stat. Phys.* **18**, 111 (1978)

[65] W. Kinzel and E. Domany, *Phys. Rev. B* **23**, 3421 (1981)

[66] L.R. Ford and D.R. Fulkerson, *Canadian J. Math.* **8**, 399 (1956)

[67] J.D. Claiborne, *Mathematical Preliminaries for Computer Networking*, (John Wiley & Sons, New York 1990)

[68] W. Knödel, *Graphentheoretische Methoden und ihre Anwendung*, (Springer, Berlin 1969)

[69] M.N.S. Swamy and K. Thulasiraman, *Graphs, Networks and Algorithms*, (John Wiley & Sons, New York 1991)

[70] L.R. Ford and D.R. Fulkerson, *Flows in Networks*, (Princeton University Press, Princeton 1962)

[71] J. Edmonds and R.M. Karp, *J. ACM* **19**, 248 (1972)

[72] E.A. Dinic, *Soviet Math. Dokl.* **11**, 1277 (1970)

[73] R.E. Tarjan, *Data Structures and Network Algorithms*, (Society for Industrial and Applied Mathematics, Philadelphia 1983)

[74] A.V. Goldberg and R.E. Tarjan, *J. ACM* **35**, 921 (1988)

[75] B. Cherkassky and A. Goldberg, *Algorithmica* **19**, 390 (1997)

[76] A.V. Goldberg, R. Satish, *J. ACM* **45**, 783 (1998)

[77] K. Mehlhorn and St. Näher, *The LEDA Platform of Combinatorial and Geometric Computing* (Cambridge University Press, Cambridge 1999); see also http://www.algorithmic-solutions.de

[78] A.A. Middleton, Phys. Rev. Lett. **88**, 017202 (2002)

[79] A.K. Hartmann and U. Nowak, *Eur. Phys. J. B* **7**, 105 (1999)

[80] J.-C. Anglès d'Auriac and N. Sourlas, *Europhys. Lett.* **39**, 473 (1997)

[81] M.R. Swift, A.J. Bray, A. Maritan, M. Cieplak, and J.R. Banavar, Europhys. Lett. **38**, 273 (1997)

[82] N. Sourlas, Comp. Phys. Comm. **121-122**, 183 (1999).

[83] U. Nowak, K.D. Usadel and J. Esser, Physica A **250**, 1 (1998).

[84] M. Gofman, J. Adler, A. Aharony, A. B. Harris, and M. Schwartz, Phys. Rev. Lett. **71**, 1569 (1993).

[85] M. Gofman, J. Adler, A. Aharony, and A.B. Harris, Phys. Rev. B **53**, 6362 (1996)

[86] K. Binder, Z. Phys. B **43**, 119 (1981)

[87] R.N. Bhatt and A.P. Young, Phys. Rev. Lett. **54**, 924 (1985); Phys. Rev. B **37**, 5606 (1988)

[88] A.A. Middleton, unpublished, preprint cond-mat/0208182

[89] S.F. Edwards and P.W. Anderson, J. de Phys. **5**, 965 (1975)

[90] B. Müller and J. Reinhardt, *Neural Networks – An Introduction*, (Spinger-Verlag, Berlin Heidelberg, 1991)

[91] G.A. Kohring, J. de Phys. I **6**, 301 (1996)

[92] R. Floriana and S. Galam, Eur. Phys. J. B **16**, 189 (2000)

[93] M. Pasquini and M. Serva, Phys. Rev. E **63** 056109 (2001)

[94] J. Maskawa, Physica A **311**, 563 (2002)

[95] G. Toulouse, Commun. Phys. **2**, 115 (1977)

[96] V. Cannella, J.A. Mydosh, Phys. Rev. B **6**, 4220 (1972)

[97] P. Norblad and P. Svendlidh, in: A.P. Young (ed.), *Spin Glasses and Random Fields*, (World Scientific, Singapore 1998)

[98] D.A. Huse, Phys. Rev. B **43**, 8673 (1991)

[99] J. Kisker, L. Santen, M. Schreckenberg, and H. Rieger, Phys. Rev. B **53**, 6418 (1996)

[100] E. Marinari, G. Parisi, F. Ricci-Tersenghi and J. J. Ruiz-Lorenzo, J. Phys. A **33**, 2373 (2000)

[101] L. Berthier and J.-P. Bouchaud, Phys. Rev. B **66**, 054404 (2002)

[102] D. Sherrington and S. Kirkpatrick, Phys. Rev. Lett. **51**, 1791 (1975)

[103] G. Parisi, Phys. Rev. Lett. **43**, 1754 (1979); J. Phys. A **13**, 1101 (1980); **13**, 1887 (1980); **13**, L115 (1980); Phys. Rev. Lett. **50**, 1946 (1983).

[104] R. Rammal, G. Toulouse, and M.A. Virasoro, Rev. Mod. Phys. **58**, 765 (1986)

[105] W.L. McMillan, J. Phys. C **17**, 3179 (1984)

[106] A.J. Bray and M.A. Moore, J. Phys. C **18**, L699 (1985)

[107] D.S. Fisher and D.A. Huse, Phys. Rev. Lett **56**, 1601 (1986)

[108] D.S. Fisher and D.A. Huse, Phys. Rev. B **38** , 386 (1988)

[109] A. Bovier and J. Fröhlich, J. Stat. Phys. **44**, 347 (1986)

[110] A.J. Bray and M.A. Moore, J. Phys. C **17**, L463 (1984)

[111] W.L. McMillan, Phys. Rev. B **30**, 476 (1984)

[112] A.K. Hartmann, Phys. Rev. E **59**, 84 (1999)

[113] B.A. Berg, U.E. Hansmann, and T.Celik, Phys. Rev. B **50**, 16444 (1994)

[114] A.K. Hartmann, Europhys. Lett. **44**, 249 (1998)

[115] E. Marinari, Phys. Rev. Lett. **82**, 434 (1999)

[116] F. Krzakala and O.C. Martin, Phys. Rev. Lett. **85**, 3013 (2000)

[117] M. Palassini and A.P. Young, Phys Rev. Lett. **85**, 3017 (2000)

[118] E. Marinari and G. Parisi, Phys. Rev. Lett. **86**, 3887 (2001)

[119] J. Houdayer and O.C. Martin, Euro. Phys. Lett. **49**, 794 (2000)

[120] H.G. Katzgraber, M. Palassini, and A.P. Young, Phys. Rev. B **63**, 184422 (2001)

[121] M. Palassini and A.P. Young Phys. Rev. B **63**, 140408(R) (2001)

[122] C.M. Newman and D.L. Stein, preprint cond-mat/0301022

[123] D.L. Stein, in T.-H. Elze (ed.), *Quantum Decoherence and Entropy in Complex Systems*, (Springer, Berlin Heidelberg 2003)

[124] E. Marinari, G. Parisi, F. Ricci-Tersenghi, J. Ruiz-Lorenzo and F. Zuliani, J. Stat. Phys. **98**, 973 (2000).

[125] C.M. Newman and D.L. Stein, Phys. Rev. B **46**, 973 (1992)

[126] C.M. Newman and D.L. Stein, Phys. Rev. Lett. **76**, 515 (1996)

[127] C.M. Newman and D.L. Stein, Phys. Rev. Lett. **76**, 4821 (1996)

[128] C.M. Newman and D.L. Stein, Phys. Rev. E **55**, 5194 (1997)

[129] C.M. Newman and D.L. Stein, in A. Bovier and P. Picco (ed.), *Mathematics of Spin Glasses and Neural Networks* (1997)

[130] C.M. Newman and D.L. Stein, Phys. Rev. E **57**, 1356 (1998)

[131] E. Marinari and G. Parisi, Phys. Rev. B **62**, 11677 (2000)

[132] F. Barahona, J. Phys. A **15**, 3241 (1982)

[133] F. Barahona, R. Maynard, R. Rammal, and J.P. Uhry, *J. Phys. A* **15**, 673 (1982)

[134] L. Saul and M. Kardar, Phys. Rev. E **48**, R3221 (1993)

[135] L. Saul and M. Kardar, Nucl. Phys. B **432**, 641 (1994)

[136] T. Regge and R. Zecchina, J. Math. Phys, **37**, 2796 (1996)

[137] S. Cho and M.P.A Fisher, Phys. Rev. B **55**, 1025 (1997)

[138] F. Merz and J.T. Chalker, Phys. Rev. B **55**, 054425 (2002)

[139] J. Bendisch, *J. Stat. Phys.* **62**, 435 (1991)

[140] J. Bendisch, *J. Stat. Phys.* **67**, 1209 (1992)

[141] J. Bendisch, *Physica A* **202**, 48 (1994)

[142] J. Bendisch, *Physica A* **216**, 316 (1995)

[143] J. Kisker, L. Santen, M. Schreckenberg, and H. Rieger, *Phys. Rev. B* **53**, 6418 (1996)

[144] N. Kawashima and H. Rieger, *Europhys. Lett.* **39**, 85 (1997)

[145] J. Bendisch, *Physica A* **245**, 560 (1997)

[146] J. Bendisch and H. v. Trotha, *Physica A* **253**, 428 (1998)

[147] M. Achilles, J. Bendisch, and H. v. Trotha, *Physica A* **275**, 178 (2000)

[148] Y. Ozeki, *J. Phys. Soc. J.* **59**, 3531 (1990)

[149] T. Kadowaki, Y. Nonomura, H. Nishimori, in: M. Suzuki and N. Kawashima (ed.), *Hayashibara Forum '95. International Symposium on Coherent Approaches to Fluctuations*, (World Scientific, Singapore 1996)

[150] R.G. Palmer and J. Adler, *Int. J. Mod. Phys. C* **10**, 667 (1999)

[151] I. Bieche, R. Maynard, R. Rammal, and J.P. Uhry, J. Phys. A **13**, 2553 (1980).

[152] U. Derigs and A. Metz, Math. Prog. **50**, 113 (1991).

[153] W.J. Cook, W.H. Cunningham, W.R. Pulleyblank, and A. Schrijver, *Combinatorial Optimization*, (John Wiley & Sons, New York 1998)

[154] B. Korte and J. Vygen, *Combinatorial Optimization - Theory and Algorithms*, (Springer, Heidelberg 2000)

[155] W.L. McMillan, Phys. Rev. B **29**, 4026 (1984)

[156] T. Shirakura and F. Matsubara, Phys. Rev. Lett. **79**, 2887 (1997).

[157] F. Matsubara, T. Shirakura, and M. Shiomi, Phys. Rev. B **58**, R11821 (1998).

[158] J. Houdayer, Eur. Phys. J. B **22**, 479 (2001)

[159] A.K. Hartmann and I.A. Campbell, Phys. Rev. B **63**, 094423 (2001).

[160] C. Amoruso, E. Marinari, O.C. Martin, and A. Pagnani, preprint cond-mat/0305042 (2003)

[161] A.C. Carter, A.J. Bray, and M.A. Moore, Phys. Rev. Lett. **88**, 077201 (2002)

[162] S. Liang, Phys. Rev. Lett. **69**, 2145 (1992)

[163] N. Kawashima, N. Hatano and M. Suzuki, J. Phys. A **25**, 4985 (1992)

[164] A very extensive review of the 2D spin glass problem has been given by N. Kawashima and T. Aoki, J. Phys. Soc. Jpn., **69**, Suppl. A, 169 (2000). See also N. Kawashima , preprint cond-mat/9910366 (1999)

[165] M. Picco, F. Ritort and M. Sales, preprint cond-mat/0106554 (2001); preprint cond-mat/0210576 (2002)

[166] Q is the probability that the value of χ^2 is worse than or equal to the current fit, i.e. a small value indicates a bad fit while $Q = 1$ means that all datapoints are straight on the fitting function. See W. H. Press, S. A. Teukolsky, W. T. Vetterling and B. P. Flannery, *Numerical Recipes in C*, Cambridge University Press, Cambridge (1995).

[167] A. A. Middleton Phys. Rev. B **63**, 060202 (2001)

[168] A.K. Hartmann and M. Moore, to be published.

[169] Information about the spin glass ground state server at the University of Köln can be found at:
`http://www.informatik.uni-koeln.de/ls_juenger/projects/sgs.html`

[170] C. De Simone, M. Diehl, M. Jünger, P. Mutzel, G. Reinelt, and G. Rinaldi, J. Stat. Phys. **80**, 487 (1995)

[171] C. De Simone, M. Diehl, M. Jünger, P. Mutzel, G. Reinelt, and G. Rinaldi, J. Stat. Phys. **84**, 1363 (1996)

[172] J. Lamarcq, J.-P. Bouchaud, O.C. Martin and M. Mézard, Europhys. Lett. **58**, 321 (2002)

[173] L. Bertier and A.P. Young, preprint cond-mat/0304576

[174] J.C. Angles d'Auriac, M. Preissmann, and A.S. Leibniz-Imag, Math. Comp. Mod. **26**, 1 (1997)

[175] A. Hartwig, F. Daske, and S. Kobe, Comp. Phys. Commun. **32** 133 (1984)

[176] T. Klotz and S. Kobe, J. Phys. A **27**, L95 (1994)

[177] T. Klotz and S. Kobe, Act. Phys. Slov. **44**, 347 (1994)

[178] T. Klotz-T and S. Kobe, in: M. Suzuki and N. Kawashima (ed.), *Hayashibara Forum '95. International Symposium on Coherent Approaches to Fluctuations*, (World Scientific, Singapore 1996)

[179] T. Klotz and S. Kobe, J. Magn. Magn. Mat. **17**, 1359 (1998)

[180] P. Stolorz, Phys. Rev. B **48**, 3085 (1993)

[181] E.E. Vogel, J. Cartes, S. Contreras, W. Lebrecht, and J. Villegas, Phys. Rev. B **49**, 6018 (1994)

[182] A.J. Ramirez-Pastor, F. Nieto, and E.E. Vogel, Phys. Rev. B **55**, 14323

[183] E.E. Vogel and J. Cartes, J. Magn. Magn. Mat. **17**, 777

[184] E.E. Vogel, S. Contreras, M.A. Osorio, J. Cartes, F. Nieto, and A.J. Ramirez-Pastor, Phys. Rev. B **58**, 8475 (1998)

[185] E.E. Vogel, S. Contreras, F. Nieto, and A.J. Ramirez-Pastor, Physica A **257**, 256 (1998)

[186] J.F. Valdes, J. Cartes, E.E. Vogel, S. Kobe, and T. Klotz, Physica A **257**, 557 (1998)

[187] H. Rieger, L. Santen, U. Blasum-U, M. Diehl, M. Jünger, and G. Rinaldi, J. Phys. A **29**, 3939 (1996)

[188] M. Palassini and A.P. Young, Phys. Rev. B **60**, R9919 (1999)

[189] D. Stauffer and P.M. Castro-de-Oliveira, Physica A **215**, 407 (1995)

[190] P. Ocampo-Alfaro and Hong-Guo, Phys. Rev. E **53**, 1982 (1996)

[191] B. A. Berg and T. Celik, Phys. Rev. Lett. **69**, 2292 (1992)

[192] B.A. Berg and T. Celik, Int. J. Mod. Phys. C **3**, 1251 (1992)

[193] B. A. Berg, T. Celik, and U.H.E. Hansmann, *Europhys. Lett.* **22**, 63 (1993)

[194] T. Celik, Nucl. Phys. B Proc. Suppl. **30**, 908

[195] B.A. Berg, U.E. Hansmann, and T.Celik, Nucl. Phys. B Suppl. **42**, 905 (1995)

[196] H. Freund and P. Grassberger, J. Phys. A **22**, 4045 (1989)

[197] N. Kawashima and M. Suzuki, J. Phys. A **25**, 1055 (1992)

[198] D. Petters, Int. J. Mod. Phys. C **8**, 595 (1997)

[199] M. Yamashita, J. Phys. Soc. Jap. **64**, 4083 (1995)

[200] Z. Michalewicz, Genetic Algorithms + Data Structures = Evolution Programs, Springer, Berlin 1992

[201] P. Sutton, D.L. Hunter, and N. Jan, J. de Phys. **4**, 1281 (1994)

[202] P. Sutton and S. Boyden, Am. J. Phys. **62**, 549 (1994)

[203] U. Gropengiesser, Int. J. Mod. Phys. C **6**, 307 (1995)

[204] U. Gropengiesser, *J. Stat. Phys.* **79**, 1005 (1995)

[205] D.A. Coley, Cont. Phys. **37**, 145 (1996)

[206] T. Wanschura, D.A. Coley, and S. Migowsky, Solid State Commun. **99**, 247 (1996)

[207] A. Pruegel-Bennett and S.L. Shapiro, Physica D **104**, 75 (1997)

[208] K. Chen, Europhys. Lett. **43**, 635 (1998)

[209] K.F. Pál, Physica A **223**, 283 (1996)

[210] K.F. Pál, Physica A **233**, 60 (1996)

[211] M. Palassini and A.P. Young, Phys. Rev. Lett. **83**, 5126 (1999)

[212] M. Palassini and A.P. Young, Proceedings of the Conference "Frontiers in Magnetism", Kyoto, October 4-7, 1999; J. Phys. Soc. Jpn. **69**, 165 (2000)

[213] M. Palassini and A.P. Young, Phys. Rev. Lett. **85**, 3333 (2000)

[214] J. Houdayer and O.C. Martin Phys. Rev. Lett. **83**, 1030 (1999)

[215] J. Houdayer and O.C. Martin, Phys. Rev. Lett. **82**, 4934 (1999)

[216] J. Houdayer and O.C. Martin, Phys. Rev. Lett. **84**, 1057 (2000)

[217] A. Sandvic, Europhys. Lett. **45**, 745 (1999)

[218] A.K. Hartmann, Europhys. Lett. **45**, 747 (1999)

[219] A.K. Hartmann, Physica A **275**, 1 (1999)

[220] J.J. Moreno, H.G. Katzgraber, and A.K. Hartmann, Int. J. Mod. Phys. C **14**, 285 (2003)

[221] A.K. Hartmann, Physica A **224**, 480 (1996)

[222] K.F. Pál, Biol. Cybern. **73**, 335 (1995)

[223] J. Hoshen and R. Kopelman, Phys. Rev. B **14**, 3438 (1976)

[224] A.K. Hartmann, Phys. Rev. E **63**, 016106 (2001)

[225] A.K. Hartmann, Phys. Rev. E **60**, 5135 (1999).

[226] K. Hukushima, Phys. Rev. E **60**, 3606 (1999)

[227] R.N. Bhatt and A.P. Young, Phys. Rev. B **37**, 5606 (1988)

[228] A.T. Ogielski and I. Morgenstern, Phys. Rev. Lett. **54**, 928 (1985); Phys. Rev. B **32**, 7384 (1985)

[229] J.D. Reger, R.N. Bhatt and A.P.Young, Phys. Rev. Lett. **64**, 1859 (1990)

[230] S. Caracciolo, G. Parisi, S. Patarnello and N. Sourlas, J.Phys.(France) **51**, 1877 (1990)

[231] N. Kawashima and N. Ito, J. Phys. Soc. Jpn. **62**, 435 (1993)

[232] E. Marinari, G. Parisi, J. Ruiz-Lorenzo, F. Ritort, Phys. Rev. Lett. **76**, 843 (1996)

[233] M.A. Moore, H. Bokil, and B. Drossel, Phys. Rev. Lett. **81**, 4252 (1998)

[234] B. Drossel, H. Bokil, M.A. Moore, and A.J. Bray, Eur. Phys. J. B **13**, 369 (2000)

[235] R.N. Bhatt and A.P. Young, J. Mag. Mag. Mat. **54-57**, 191 (1986)

[236] G. Hed, A. K. Hartmann and E. Domany, Europhys. Lett. **55**, 112 (2001).

[237] G. Hed, A. K. Hartmann, D. Stauffer and E. Domany, Phys. Rev. Lett., **86**, 3148 (2001)

[238] E. Marinari and G. Parisi, Europhys. Lett. **19**, 451 (1992)

[239] K. Hukushima and K. Nemoto, J. Phys. Soc. Jpn. **65**, 1604 (1996)

[240] D.A. Huse and D.S. Fisher, J. Phys. A **20**, L997 (1987)

[241] E. Marinari, G. Parisi, F. Ricci-Tersenghi, and J.J. Ruiz-Lorenzo, J. Phys. A **31** L481, (1998).

[242] D.J. Gross and M. Mezard, Nuclear Physics B **240** [FS12], 431 (1984)

[243] F. Krzakala and O.C. Martin, Europhys. Lett. **53**, 749 (2001)

[244] T. Hogg, B.A. Huberman and C. Williams (eds.), Frontiers in problem solving: phase transitions and complexity, *Artif. Intell.* **81** (I+II) (1996)

[245] B. Hayes, *Am. Scient.* **85**, 108 (1997)

[246] O. Dubois, R. Monasson, B. Selman and R. Zecchina (eds.), special issue of J. Theor. Comp. Sci. **265** (2001)

[247] D. Mitchell, B. Selman and H. Levesque, in *Proc. 10th Natl. Conf. Artif. Intell. (AAAI-92)*, 440 (AAAI Press/MIT Press, Cambridge, Massachusetts, 1992)

[248] B. Selman and S. Kirkpatrick, Science **264**, 1297 (1994)

[249] N. Goldenfeld, *Lectures on Phase Transitions and the Renormalization Group*, (Addison Wesley, Reading, MA, 1992)

[250] M. Mézard, G. Parisi and M.A. Virasoro, *Spin glasses and beyond*, (World Scientific, Singapore 1987)

[251] S.A. Cook, Proc. 3rd ACM Symp. on the Theory of Computing, 151 (Association for Computer Machinery, New York, 1971)

[252] S.A. Cook, *J. Assoc. Comput. Mach.* **18**, 4-18 (1971)

[253] R. Monasson, R. Zecchina, Phys. Rev. E **56**, 1357 (1997)

[254] R. Monasson, R. Zecchina, S. Kirkpatrick, B. Selman and L. Troyansky, Nature **400**, 133 (1999)

[255] G. Biroli, R. Monasson and M. Weigt, Europ. Phys. J. B **14**, 551 (2000)

[256] F. Ricci-Tersenghi, M. Weigt and R. Zecchina, Phys. Rev. E **63**, 026702 (2001)

[257] M. Mézard, G. Parisi and R. Zecchina, Science **297**, 812 (2002)

[258] P. Erdös and A. Rényi, Publ. Math. Inst. Hung. Acad. Sci. 5,17 (1960)

[259] J. Harant, Discr. Math. 188, 239 (1998)

[260] C. Caro, Technical Report, Tel Aviv University (1979)
V. K. Wei, Bell Lab. Technical Memorandum 81-11217-9 (1981)

[261] P. G. Gazmuri, Networks 14, 367 (1984)

[262] A. M. Frieze, Discr. Math. 81, 171 (1990)

[263] E. Balas and A. Samuelson, Management Sci. Res. Rep. **325**, (Carnegie-Mellon Univ., Pittsburgh, PA, 1973)

[264] G.L. Nemhauser and L.E. Trotter, Math. Programming **8**, 232 (1975)

[265] R.E. Tarjan and A.E. Trojanowski, SIAM J. Comp. **6**, 537 (1977)

[266] M. Bauer and O. Golinelli, Eur. Phys. J. B **24**, 339 (2001)

[267] M. Shindo and E. Tomita, Syst. Comp. Jap. **21**, 1 (1990)

[268] E.L. Lawler and D.E. Wood D E, Oper. Res. **14**, 699 (1966)

[269] R. Lüling and B. Monien, Sixth International Parallel Processing Symposium, IEEE Comput. Soc. Press, Los Alamitos, USA, 543 (1992)

[270] A.K. Hartmann and M. Weigt, J. Theor. Comp. Sci. **265**, 199 (2001)

[271] B. Bollobas, *Random Graphs* (Academic Press 1985)

[272] R.J. Baxter, *Exactly Solved Models in Statistical Mechanics*, (Academic Press London, 1982)

[273] F.M. Russo, Phys. Lett. A **239**, 17 (1998)

[274] S. Scarpetta, A. de Candidia and A. Coniglio, Phys. Rev. E **55**, 4943 (1997)

[275] F. Ricci-Tersenghi, D.A. Stariolo, J.J. Arenzon, Phys. Rev. Lett. **84**, 4473 (2000), Phys. Rev. E **62**, 5978 (2000)

[276] M. Nicodemi, A. Coniglio and H.J. Herrmann, Phys. Rev. E **55**, 3962 (1997); J. Phys. A **30**, L379 (1997)

[277] M. Nicodemi J. Phys. **I7**, 1365 (1998)

[278] E. Caglioti, H.J. Herrmann, V. Loreto and M. Nicodemi, Phys. Rev. Lett. **79**, 1575 (1997)

[279] M. Nicodemi and A. Coniglio, Phys. Rev. Lett. **82**, 916 (1999), J. Phys. C **12**, 6601 (2000)

[280] R. Monasson and O. Pouliquen, Physica A **236**, 395 (1997)

[281] A. Barrat and V. Loreto, J. Phys. A **33**, 4401 (2000)

[282] R. Monasson, J. Phys. A **31**, 513 (1998)

[283] C. De Dominicis and P. Mottishaw, J. Phys. A20, L1267 (1987)

[284] P. Mottishaw and C. De Dominicis, J. Phys. A20, L375 (1987)

[285] K.Y.M. Wong and D. Sherrington, J. Phys. A21, L459 (1988)

[286] Y.Y. Goldschmidt and P.Y. Lai, J. Phys. A23, L775 (1990)

[287] M. Mézard and G. Parisi, Eur. Phys. J. B **20**, 217 (2001)

[288] H. Zhou, preprint cond-mat/0302289 (2003)

[289] M. Bauer and O. Golinelli, Phys. Rev. Lett. **86**, 2621 (2001)

[290] S. Cocco and R. Monasson, Phys. Rev. Lett. **86**, 1654 (2001)

[291] M.T. Chao and J. Franco, SIAM J. Comput. **15**, 1106 (1986)

[292] M.D. Davis, R. Sigal, and E.J. Wyuker, *Computability, Complexity and Languages*, (Academic Press, San Diego 1994)

[293] C.H. Papadimitriou and K. Steiglitz, *Combinatorial Optimization*, (Dover Publications, Mineola (NY) 1998)

Selected orginial research contributions involving the author